Hydrobiologia (2019) 842:191–217
https://doi.org/10.1007/s10750-019-04036-9

PRIMARY RESEARCH PAPER

Effects of nutrient limitation, salinity increase, and associated stressors on mangrove forest cover, structure, and zonation across Indian Sundarbans

Rajojit Chowdhury · Tapan Sutradhar · Mst. Momtaj Begam · Chandan Mukherjee · Kiranmoy Chatterjee · Sandip Kumar Basak · Krishna Ray

Received: 23 January 2019 / Revised: 12 July 2019 / Accepted: 25 July 2019 / Published online: 3 August 2019

Abstract Anthropogenic coastal activities and natural stressors aggravate degradation of small coastal patches of mangroves, which in turn destroy local resilience of mangrove forests in the Indian Sundarbans, the continuous mangrove habitat that spans between India and Bangladesh. We conducted an analytical survey across 19 shoreline mangrove fringes spanning the Sundarbans, including both healthy and disturbed forests, and evaluated ninety-five 60-cm composite sediment cores across a degradation and salinity gradient from ~ 4 to ~ 12 ppt. Increased salinity and anoxicity greatly inhibited nutrient cycling and release by microbial decomposers, subsequently resulting in nutrient-poor soil as a condition of degradation. Nutrient limitation, salinity rise, anoxicity increase, and sulfide build-up negatively controlled forest structure causing declines of forest coverage from ~ 98 to ~ 11%. In addition, the tide-dominated salinity gradient controlling species zonation was disrupted in disturbed forests with salinity-sensitive species gradually disappearing. An obvious change in species distribution is anticipated while salt-sensitive *Heritiera fomes*, *Xylocarpus* spp., and *Phoenix paludosa* failed to cope with increased salinity, evident by their absence from many forests. *Excoecaria agallocha* and *Avicennia* spp. acclimated well and expanded freely into degraded forests across the Sundarbans. Overall, our study strongly

Handling editor: K. W. Krauss

Rajojit Chowdhury and Tapan Sutradhar have contributed equally to this work.

Electronic supplementary material The online version of this article (https://doi.org/10.1007/s10750-019-04036-9) contains supplementary material, which is available to authorized users.

R. Chowdhury · T. Sutradhar · Mst. M. Begam · C. Mukherjee · K. Ray (✉)
Environmental Biotechnology Group, Department of Botany, West Bengal State University, Berunanpukuria, Malikapur Barasat, Kolkata 700126, India
e-mail: kray91@gmail.com

S. K. Basak (✉)
Sarat Centenary College, Dhaniakhali, Hooghly, West Bengal 712302, India
e-mail: sandipbasak9592@gmail.com

K. Chatterjee
Department of Statistics, Bidhannagar College, Salt Lake City, Sector 1, Block EB, Kolkata 700064, India

establishes salinity intrusion as primary mechanism for mangrove degradation.

Keywords Nutrient limitation · Forest cover · Salinity rise · Nutrient cycling enzymes · Mangrove zonation · Species occurrence · Salinity gradient

Introduction

Globally, up to 35% of the mangrove area has been lost since the 1980s, primarily due to different coastal development activities (Curnick et al., 2019). Recently, great concern has been expressed over the loss and degradation of relatively small coastal patches of mangroves (Curnick et al., 2019). These patches are reported to be very important to low-lying island nations vulnerable to climate change and sea level rise, and their continued loss and fragmentation create barriers to species movement and dispersal, destroy local coastal resilience, and drive key mangrove ecosystems towards collapse (Curnick et al., 2019). The Indian Sundarbans encompasses a part of the contiguous mangroves that stretch between India and Bangladesh. The Sundarbans was declared a Ramsar site under the Ramsar Convention in 1992, and UNESCO proclaimed Sundarbans as a World Heritage Site in 1997 (Sarker et al., 2016). A large area of Indian Sundarbans is protected by the Sundarban Biosphere Reserve (SBR); however, isolated mangrove forests distributed among various islands in the SBR suffer from continuous degradation. The river shorelines in the Indian Sundarbans that are typically fringed by mangroves are extremely vulnerable to anthropogenic stresses, such as deforestation, dredging, infrastructure development catering to tourism, reconstruction of sea dykes and embankments through the use of dredged sand and mud from river shoreline and mudflat zones, prawn larvae catching, and fish farming along the shoreline.

Dredge spoils are often dumped along river edges beyond tidal influence and then abandoned, thus killing the shoreline mangroves through burial and smothering by the dredgers. Spoils adjacent to the mangrove stands predispose these areas to sediment degradation by wastes and refuse from fish farming and construction operations. These activities expose the mangrove sediment to potential infiltration of organic wastes, toxicants viz. antifoulant tributyltin (TBT), additives including stabilizers (fatty acid salts), pigments (chromates, cadmium sulfate), antioxidants (hindered phenols), UV absorbers (benzophenones), flame retardants (organophosphates), pesticides, antibiotics, fungicides, and disinfectants (GESAMP, 1991). Re-colonization of these sites by native species has not been observed. In an Indian government-run project, the covering of the riverside slope with polypropylene sheets, a non-biodegradable material, to control erosion proved extremely detrimental to the survival of shoreline mangrove ecosystems in the Indian Sundarbans (The Hindu Business Line, 2012 updated in 2017 by Press Trust of India). This project destroyed the habitats of flora and fauna in the shoreline area, affected the sediment fertility, and affected the microbe-mediated nutrient cycling process, which is essential for mangrove growth. Apart from anthropogenic stressors, natural stressors (e.g., frequent cyclonic storms, increased salinity, sea level rise, and shoreline erosion) also pose major threats by causing the decline of mangrove fringes in Indian Sundarbans.

Soil nutrient availability is an important determinant in the spatial distribution of vegetation (Vince & Snow, 1984). The concentrations of organic carbon, ammonia–nitrogen, and plant-available phosphorus and the activity of microbial enzymes for decomposition and nutrient cycling in sediments can be critical decisive factors controlling the density and development of mangrove forests. The availability of essential macronutrients in the mangrove sediments has been critical for the understanding of mangrove growth patterns (Boto & Wellington, 1984; Medina, 1984; Medina et al., 2001; McKee et al., 2002; Feller et al., 2003; Marchand et al., 2004; Lovelock et al., 2006; López-Hoffman et al., 2007) and the structure and productivity of mangrove forests (McKee, 1995; Chen & Twilley, 1999; Reef et al., 2010). Most investigations of mangrove nutrient limitations have emphasized the macronutrients N and P, which are the nutrients most likely limiting the primary productivity and growth in mangrove ecosystems (Krauss et al., 2008). An experimental study conducted on mangroves in North Queensland, Australia indicated iron deficiency was a limiting factor (Alongi, 2010). Nutrient supply in mangrove forest sediments typically comes from riverine inputs via tidal flushes, runoff from the terrestrial landward side, and the

decomposition of litter and other detritus by soil microbial organisms (Cannicci et al., 2008). Any hindrance to these three processes resulting from anthropogenic activities or natural stressors adversely affects the nutritional balance of the sediments. Nutrient limitation could also threaten the ecological balance within mangrove ecosystems (McKee et al., 2002; Feller et al., 2003). It was observed in the Shark River estuary in Florida, USA, that the decrease in sediment fertility could cause landward decline of mangrove basal area and biomass (Chen & Twilley, 1999). Nutrient availability may also influence mangrove vegetation performance in Africa (Ukpong, 1997). The concentrations of organic carbon, P, Ca, Mg, and K in mangrove forest sediments in Nigeria could be correlated with individual species coverage (Ukpong, 2000). These aforementioned studies all point towards a possible link between nutrient status of the sediments and mangrove forest coverage.

Apart from nutrient limitations, anoxic soil conditions, which are typical for mangrove systems, are associated with modification of soil-chemical processes with sulfate reduction by sulfate reducing bacteria, resulting in the accumulation of sulfides that are potentially toxic to plants (Nickerson & Thibodeau, 1985). The growth of mangroves depends on mechanisms for detoxification of sulfides or acclimation to sulfide-rich environments under increasing anoxicity. In addition, excessive soil salinity could also be a causal factor in limiting mangrove growth (Bompy et al., 2014). Sediment salinity fluctuations occur in mangrove forests due to tidal inundation, sea level rise, variable annual precipitation, and soil surface evaporation with temperature rise (Hutchings & Saenger, 1987). However, in the Indian Sundarbans, the salinity increases in mangrove forest sediments is not limited to these criteria alone. The steady rise in riverine water salinity is considered a result of reduced freshwater flow from the Ganges' into the Sundarbans from 3700 to 364 $m^3 s^{-1}$ since the construction of the Farakka Dam in India in 1974 (Sarker et al., 2016). The Ganges has silted up most of its southbound distributaries heading towards the Sundarbans' river system with an approximately 60% reduction in the freshwater flow (Sarker et al., 2016). Although erosion and accretion are both associated with delta forming processes, erosion has left a severe impact on the islands of Indian Sundarbans. The sea-facing islands in southern Sundarbans are the most vulnerable to erosion (Center for Science and Environment, India, 2012). This erosion process, along with gradual tidal invasion, has jeopardized the existence of lower intertidal mangrove communities.

Mangroves are usually naturally organized into rather predictable monospecific zones parallel to shorelines, resulting in virtual zonation, a widely recognized feature of mangrove forests (Lugo & Snedaker, 1974). These zonation patterns are an expression of plant succession or a physiological response to tide-maintained salinity gradients (Snedaker, 1982). The growth responses of mangroves across this landward–coastward salinity gradient reflect a physiological continuum of salinity tolerance ranging from moderately salt-tolerant glycophyte to those of highly salt-tolerant and apparently obligate halophytes (Ball, 1988). Due to any perturbation in tide-controlled salinity gradient, this specific zonation of mangrove species in a forest becomes highly vulnerable to change. With the rising salinity gradient, both species composition and distribution along a gradient from coastal to interior land may proceed towards a gradual change. Salinity increases can even lead to decreases in the distribution of some low-salinity loving species or simultaneous increases in more salt-tolerant species (Payo et al., 2016).

Under the above scenario of anthropogenic influences and natural stressors, together having high possibility of impacting mangrove sediments in terms of nutrient availability, rising salinity, and anoxicity, we conducted an analytical survey across 19 mangrove forests in the western part of Indian Sundarbans. We hypothesized that the nutrient availability in mangrove sediments that controls the sediment fertility would affect the corresponding mangrove forest cover and structure. The zonation pattern of mangrove species in each forest was also studied along salinity gradient transects. We hypothesized that this study would reveal variation in the salinity of the native habitat of mangrove species across different forests situated at the shoreline fringes and demonstrate the relative position of occurrence of mangroves across different forests spanning between the river's edge and the landward side.

Materials and methods

Study area

Our study is based on small shoreline mangrove forests in the Indian Sundarbans, India. We noticed that some of the shoreline mangrove forests are typically affected by the described stressors. We preliminarily identified these forests on the basis of visual impression only made from the field in terms of vegetation density and apparent thinning. We also compared Google Earth images for each forest to evaluate the apparent forest cover status at each location (Fig. 1). We initially judged the forests based on these images (Fig. 1) and our physical verification made in the field. We wanted to compare the degradation criteria (e.g., physical and chemical characterization of sediments and forest structure and cover analyses of the affected mangrove forests) with that of other mangrove forests in this region that are comparatively protected from anthropogenic effects. Altogether, 19 small mangrove forests in Indian Sundarbans were studied, and we present here a comparative account of these forests from the viewpoint of the physical and nutritional profile of the sediment and the forest cover and structure associated with the effects of varying habitat salinity and prevailing erosion on the shoreline mangrove community.

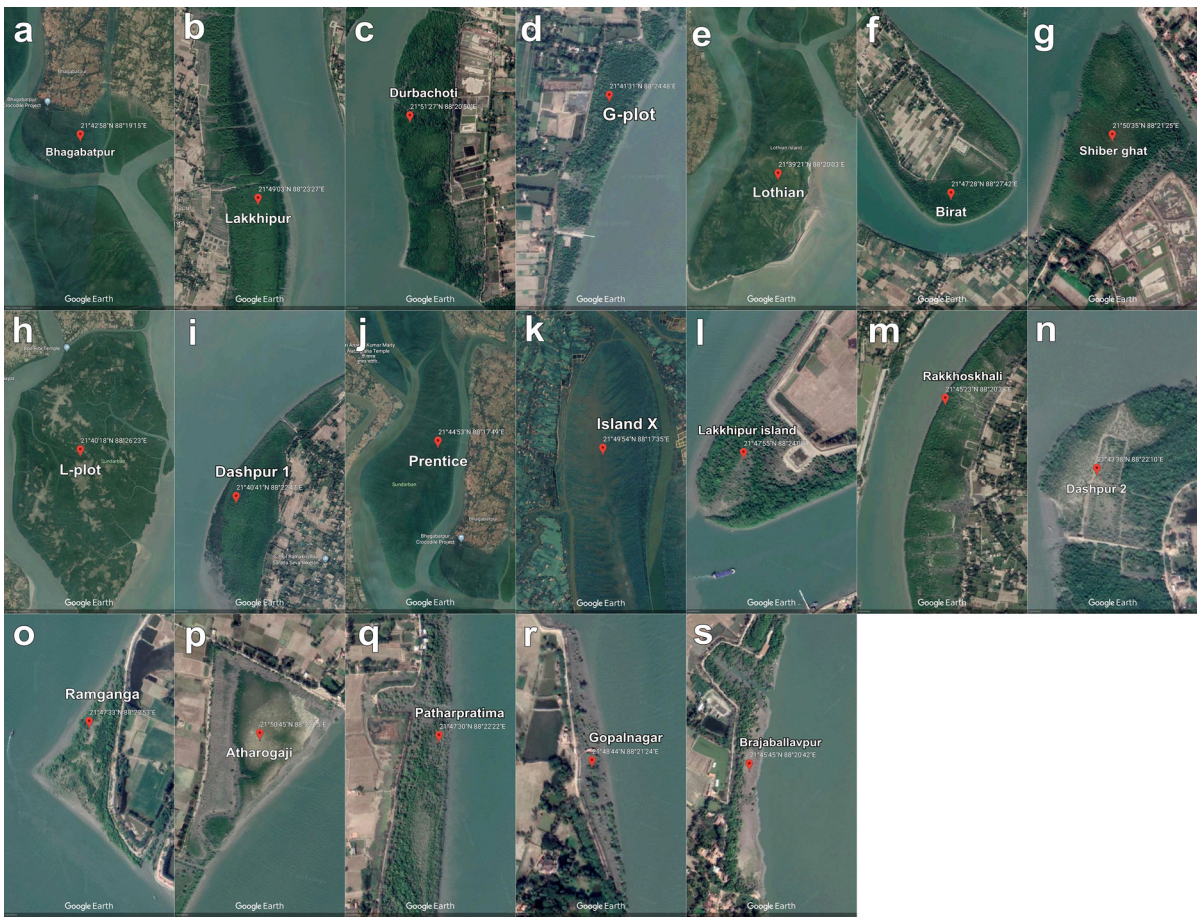

Fig. 1 Aerial imagery from Google Earth for the 19 small forests studied in the western Indian Sundarbans, India: **a** Bhagabatpur, **b** Lakkhipur, **c** Durbachoti, **d** G-Plot, **e** Lothian, **f** Birat, **g** Shiber Ghat, **h** L-plot, **i** Dashpur 1, **j** Prentice, **k** Island X, **l** Lakkhipur island, **m** Rakkhoshkhali, **n** Dashpur 2, **o** Ramganga, **p** Atharogaji, **q** Patharpratima, **r** Gopalnagar, and **s** Brajaballavpur. All forests studied were located on shoreline fringes. These aerial images provided a preliminary assessment of apparent forest cover status prior to selection for this study

Our study spans the area between 21°40′0″N to 22°0′0″N and 88°20′0″E to 88°30′0″E in the western part of Indian Sundarbans, as observed in Fig. 2. The entire studied area is located on the shorelines of an intricate network of river systems and creeks: Sutarbag, Mridangabhanga, Calchara, Curzon Creek, Saptamukhi, Saralda Khal, Barchara, Walsh Creek, and Rakshakhali Khal. The studied forests are named according to their locations. The Lakkhipur, Bhagabatpur, Lothian, G-Plot, and Durbachoti mangrove forests seemed to be the healthiest forests least disturbed by anthropogenic interventions, and we considered these forests as our standard controls in this study. The other studied mangrove forests were observed to be at various states of degradation from moderately disturbed to exceedingly disturbed and patchy degraded forms as judged by their visual appearance (Fig. 1). The locations of all the surveyed forest sites and soil sampling sites are shown in Fig. 2. The distribution of the forests and their corresponding percent cover values are also displayed in Fig. 3.

Soil sampling

In each of the 19 mangrove forests, five 100 m^2 randomly laid quadrats (Fig. 4a) were established in the upper, middle, and lower intertidal zones. Ten sediment cores (60 cm long and 4 cm wide) were collected from each quadrat, divided into four parts according to the sub-soil depths of 0–15 cm, 15–30 cm, 30–45 cm, and 45–60 cm, and then mixed into one composite sample (Carter & Gregorich, 2008) for each depth. Hence, from each forest, we collected five composite samples (including four sub-soil samples from each) for analysis. Samples were collected during both dry (summer) and wet (monsoon) seasons during 2014–2017. It took four years to collect cores across all 19 forests covering both dry and wet seasons. A total of 950 initial cores (50 per forest) were collected, of which 95 composite cores (5 per forest including four sub-soils from each) were analyzed. Each composite sediment sample was analyzed in three depth wise replicate sets. The samples were kept in an ice box during transport to the laboratory. One part of each sediment sample was kept at 4°C for assay of the activity of nutrient cycling enzymes and sulfide content. The rest of the sample was air-dried at room temperature (28°C) and analyzed for chemical and physical properties. Tidal water was also collected from the 19 forests during the summer and monsoon seasons to record water salinity.

Chemical and physical analyses of sediments

Sediment samples from each depth (0–15 cm, 15–30 cm, 30–45 cm, and 45–60 cm) were analyzed separately. Ammonia-N was assayed by extracting 2 g of sample with 2 M KCl (Dorich & Nelson, 1983), and the concentration was determined by the phenate method. The developed indophenol blue color (Solórzano, 1969; Dorich & Nelson, 1983; Park et al., 2009) was measured after 1 h with a spectrophotometer at 640 nm. For plant-available phosphorus, 2 g of sample extracted with modified Morgan extractant (McIntosh, 1969) was tested for soluble phosphorus by the molybdenum-blue method (Krishnaswamy et al., 2009). Organic carbon was determined by reacting 1 g of sediment with 1/6 M potassium dichromate ($K_2Cr_2O_7$) and concentrated sulfuric acid containing 1.25% silver sulfate (Ag_2SO_4) (Datta et al., 1962). The suspension developed a green color when incubated for 30 min, and the color intensity was measured at 660 nm. For sulfide assays, 2.5 g of fresh sediment was reacted for the liberation of sulfide by phosphoric acid steam distillation. The distillate was treated with DPD sulfuric acid reagent, and following the addition of potassium dichromate solution, the absorbance of the resulting blue color was measured at 670 nm to estimate the sulfide-sulfur content (Environment Agency, UK, 2010).

CMC-cellulase activity was determined with 1 g of fresh sample that was incubated with toluene and reacted with 0.5% carboxy methyl cellulose (CMC) in acetate buffer (50 mM, pH 5.5). After incubation at 30°C for 48 h, the CMC-cellulase activity was determined by the Somogyi–Nelson method (Deng and Tabatabai, 1994), with controls designed so that they allowed for the subtraction of the native soil reducing sugars and any trace amount of reducing sugars produced by the chemical hydrolysis of CMC during the incubation period. CMC-cellulase units were estimated as mg of glucose kg^{-1} 24 h^{-1}. Alkaline and acid phosphatase activity of the sediment samples were determined with 1.5 g of fresh soil reacted with 0.05 M *para*-nitrophenyl phosphate (*p*NPP) (Verchot & Borelli, 2005). The process released the product yellow-colored *para*-nitrophenol (*p*NP) from the substrate, and the color intensity was measured at 410 nm.

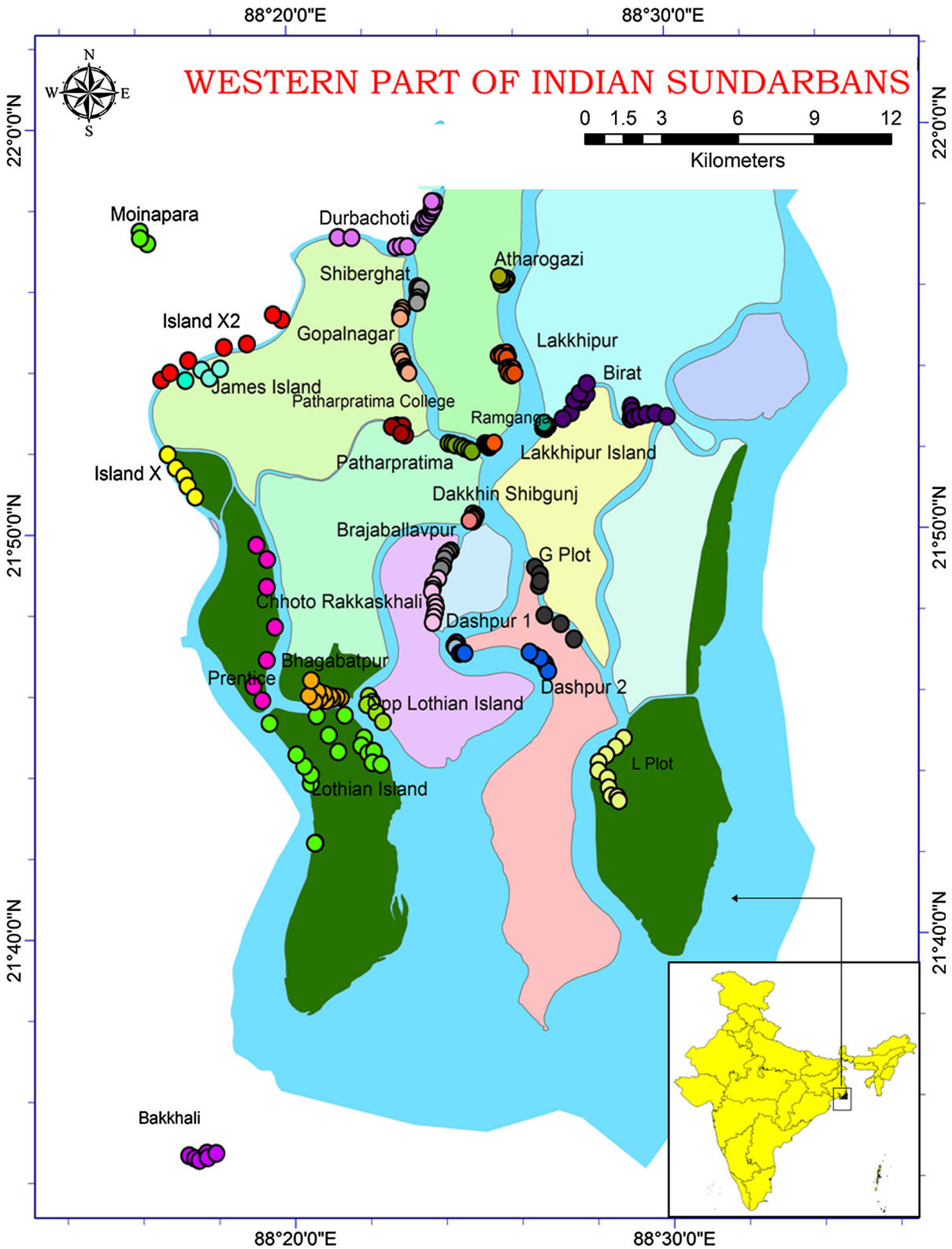
WESTERN PART OF INDIAN SUNDARBANS
88°20'0"E
88°30'0"E
22°0'0"N
21°50'0"N
21°40'0"N
N
S
E
W
0 1.5 3 6 9 12
Kilometers
Moinapara
Durbachoti
Atharogazi
Shiberghat
Island X2
Gopalnagar
Lakkhipur
Birat
James Island
Patharpratima College
Ramganga
Lakkhipur Island
Patharpratima
Island X
Dakkhin Shibgunj
Brajaballavpur
G Plot
Chhoto Rakkaskhali
Dashpur 1
Bhagabatpur
Prentice
Dashpur 2
Lothian Island
L Plot
Bakkhali

◀**Fig. 2** Map of study area within the western Indian Sundarbans, India, illustrating the locations of the 19 mangrove forests with sediment sampling sites. Study sites of different forests are identified by different colors for sediment sampling. All locations were positioned on the river shoreline, which is indicated by blue color. Sampling sites for sediment collection often are coincident with sites for forest structure survey. Points show aggregation and overlapping due to closely positioned locations. Deep green color islands are protected areas under Sundarban Biosphere Reserve

Enzyme activity units were calculated based on mmol of *p*NP released kg^{-1} h^{-1}. To assay β-glucosidase activity, 1.5 g of fresh sample was dissolved in 0.05 M acetate buffer (pH 5), and the slurry was reacted with *p*NP-*b*-D-glucopyranoside (0.005 M). After 2 h of incubation, 1 N NaOH was added to the clear supernatant. The color intensity was measured at 410 nm (Verchot & Borelli, 2005). The units were calculated as mmol of *p*NP released kg^{-1} h^{-1}. For aryl sulfatase activity, 0.5 g of air-dried sample in toluene was incubated at 20°C for 1 h and then reacted with 0.5 M acetate buffer at pH 5.8 and 0.05 M *para*-nitrophenyl sulfate at 37°C for 1 h. Activity was determined by spectrophotometry at 400 nm by measuring the yellow-colored *para*-nitrophenol (*p*NP) released from the *p*-nitrophenyl sulfate (Whalen & Warman, 1996). The enzyme units were evaluated as mg of *p*NP released kg^{-1} h^{-1}. Urease was assayed by dissolving 2.5 g of fresh sample in 0.08 M urea solution and adding Na salicylate/NaOH and 0.1% Na dichloroisocyanurate to the clear filtrate after 2 h of incubation. Absorbance was measured at 690 nm after 30 min of incubation (Kandeler & Gerber, 1988). The units of urease were formulated as mg of ammonia–nitrogen released kg^{-1} h^{-1}. Because oxygen constraints and anoxic conditions are common in mangrove environments, we decided to use phenol oxidase activity as an indicator of oxygen constraints in the sediment layers (0–60 cm). Phenol oxidase was determined by oxidation of L-DOPA. One gram of fresh sediment was dissolved in bicarbonate buffer (pH 8) to prepare a soil slurry that was mixed with 8 mM L-DOPA (prepared with 0.1 M citrate buffer, pH 4.8), which was then incubated for 3 h at 20°C. The supernatant was measured for absorbance at 475 nm (Gallo et al., 2004; Bach et al., 2013). The units of phenol oxidase activity were calculated as mmol of dopachrome released kg^{-1} h^{-1}. All the spectrophotometric analyses were performed using a SmartSpec Plus spectrophotometer (Bio-Rad, California, USA).

The conductivity of the sediment samples was measured using the method of fixed ratio saturated extract preparation in the proportion of 1:2 (w/w, air-dried sediment: deionized water) (Janzen, 1993; Rhoades, 1996) and shaken for 1 h. The conductivity of the suspension was measured by conductivity meter (Chemiline CL250, Labline Technology Pvt. Ltd., Ahmedabad, India) and conductivity was expressed as salinity in ppt. Similarly, the salinity of the tidal water from each of the 19 mangrove forests was directly measured by the conductivity meter and salinity was expressed in ppt. The pH was determined using a pH meter (Chemiline, Labline Technology Pvt. Ltd., Ahmedabad, India). The sand, silt, and clay percentages of the sediments were determined using sieves of different pore size according to Kettler et al. (2001).

Evaluation of mangrove forest structure

Ten quadrats, each measuring 10 m × 10 m, were used to study forest structure at different positions within each forest site. Additionally, five of these quadrats from each forest were also used for sediment core collection. The circumference above the base (1.4 m above the ground) was measured for each tree and shrub species. The diameter at breast height (DBH) and tree basal area (TBA) were calculated using standard formulae from the measured circumference (Etigale et al., 2014). The forest cover percentage for each species was calculated after multiplying the average TBA by the total number of individuals of that species present in all quadrats in a certain mangrove forest. The total forest cover for each forest was accordingly determined by combining the coverage areas of all the constituent species in a forest. For each species, the density, frequency, and dominance in each forest were determined (Curtis & McIntosh, 1950). We calculated the importance value index (IVI) (Cottam & Curtis, 1956) for the ten dominant mangrove species inhabiting these forests. The IVI was calculated as the sum of the relative density, relative frequency and relative dominance of a particular species in each forest (Cottam & Curtis, 1956). The maximum composite IVI of any forest is 300, obtained by combining the IVI values of all component species (Campo et al., 2018).

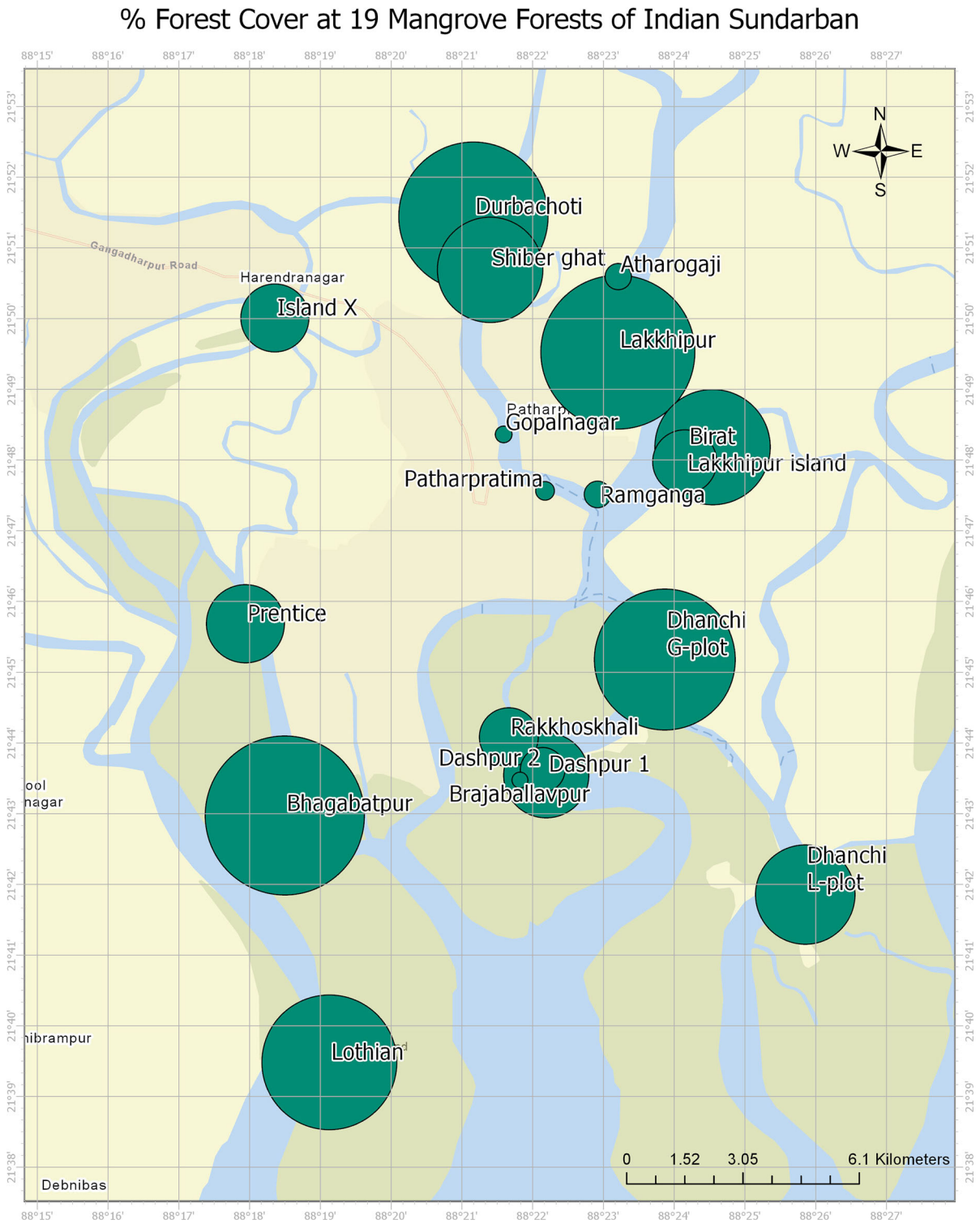
% Forest Cover at 19 Mangrove Forests of Indian Sundarban
N
W
E
S
Durbachoti
Shiber ghat
Atharogaji
Harendranagar
Island X
Lakkhipur
Gopalnagar
Birat
Lakkhipur island
Patharpratima
Ramganga
Prentice
Dhanchi
G-plot
Rakkhoskhali
Dashpur 2
Dashpur 1
Brajaballavpur
Bhagabatpur
Dhanchi
L-plot
Lothian
Debnibas
0 1.52 3.05 6.1 Kilometers

◀**Fig. 3** Forest cover (%) map for each of the 19 forests surveyed across the Indian Sundarbans, India. Forest cover represented by scaled dots, with each green circle indicating the percent cover. The bigger the circle, the higher the forest cover. The forest cover ranged between ∼ 98 and ∼ 11%. The forests were located on the shoreline fringes at the backdrop of an intricate river network shown by blue color. Light green color islands are protected areas under Sundarban Biosphere Reserve

Evaluation of the relative occurrence of mangroves across the salinity gradient

Five transects, each 100 m long and 10 m wide, were laid out perpendicular to the shoreline from the river's edge towards the furthest inland point (Fig. 4b) in each forest to record the locations of first appearance of each species along the transects. This survey was repeated three times per forest to minimize the error rates. The relative occurrence of each species was denoted by a score calculated as the distance of the species' location from the river's edge along a transect divided by the total distance covered by the respective transect. The distances covered by the transects were identical (i.e., 100 m). Thus, the relative occurrence values were less than or equal to 1. For a particular species in a forest, the relative occurrence values obtained from different transects were averaged, and the standard deviation was calculated. This method of determining the relative occurrence of mangrove species was based on the previously described species sequencing method (Williams et al., 1991; Bunt et al., 1991). In addition to species relative occurrence, sediment cores were collected from the sites where the species were located along the transects. Sediment cores were later analyzed for salinity. The number of sediment cores varied among transects (6–10 per transect) and was dependent on the number of species locations along a transect. The core collection points were spatially separated in riverward–landward direction and cores were collected from the region where a species showed maximal density (considered as native habitat of the species) along a transect within 100 m. Cores were numbered in increasing order from riverside to inland positions with dimension as 60 cm long and 4 cm wide. Salinity of the individual core sample was analyzed by the earlier described method (Janzen, 1993; Rhoades, 1996). The transect records generated in this study were not time-series data. We collected these data only by surveying the 19 forests and repeated the process thrice to reduce any observational error. A score for each species that denoted the relative position of occurrence of the species from the river's edge to the landward side was determined for each of the 19 forests. The salinity data were generated along the transects at the site of species occurrence in each forest. Graphical representations were prepared for further analyses in which the species' relative occurrence scores across the transects spanning from river's edge to the landward side were plotted against the corresponding habitat salinity.

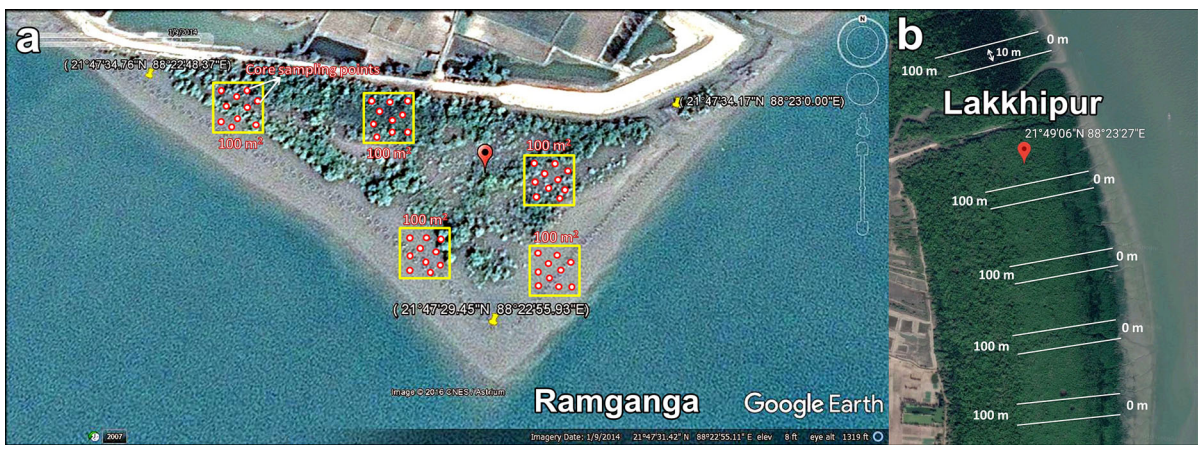

Fig. 4 Schematics illustrating the design of sediment cores collection at the level of a single forest. **a** Sediment sampling within five randomly laid quadrats. **b** Sediment sampling along five transects laid perpendicular to the shoreline and extending towards riverward-landward direction

Statistical analyses

The mean value ± standard error was considered for all analyses of sediment variables. Analysis of variance (ANOVA) along with Tukey's honest significant difference (HSD) test were used to determine if there were significant differences in the measured parameters across the forests and across the different sediment depths. Values designated with different letters are significantly different at the 5% level according to Tukey's HSD test. Two sample *t* test at 95% significance level was done to understand the differences in the values obtained with two treatment groups viz. values of variables obtained from dry and wet seasons with GraphPad Prism 5.0 software. All the sediment parameters from the four studied depths were evaluated for correlations with forest coverage from the 19 mangrove forests using Pearson's correlation coefficient analyses with SYSTAT version 13 software. Finally, principal component analysis (PCA) was performed in SPSS 23.0 software to holistically ascertain the relationships among all physical and chemical variables measured in the mangrove sediments. The PCA plots were created considering the factors that explained the maximum amount of the cumulative variance within the datasets.

Results

Physical and chemical properties of mangrove sediments across varying levels of forest cover

Sediments from 19 mangrove forests were evaluated in terms of their physical properties, namely sand, silt and clay percentage, pH and salinity, and chemical properties, namely ammonia-N, plant-available phosphorus (P), soil organic carbon (SOC), and sulfide, and activities of soil microbial enzymes, such as arylsulfatase, CMC-cellulase, β-glucosidase, alkaline and acid phosphatase, urease, and phenol oxidase. Data for these variables were collected from both dry and wet seasons, but negligible variation was observed between seasons except for tidal water salinity (Supplementary Files 2 and 3). We performed *t* tests between data obtained in dry and wet seasons for all the sediment variables and for tidal water salinity from all sites. Except for tidal water salinity, our results did not show significant difference between dry and wet seasons (Supplementary File 3). Nutrients and microbial enzymes did not show significant difference in values obtained for dry and wet seasons with a few exceptions for physical properties of the sediments (Supplementary File 3).

The analyses revealed that for sand, silt, clay, sediment pH, and sediment salinity, there were no significant variations across the four soil depths (Table S1 and Figs. 5, S1). For sediment pH, the values only ranged between 7 and 8 across the 19 forests (Table S1). Tidal water salinity ranged within 10–28 ppt with significant variation within dry and wet seasons (Table S1, Supplementary File 3). Variables such as ammonia-N, plant-available P, and SOC showed the highest values in the topmost layer of 0–15 cm depth, and each of the variables progressively decreased at greater depths of 15–30, 30–45, and 45–60 cm in each forest (Table S2 and Figs. 6a–c, S2a, S2b, S2c), except for sulfide. For sulfides, deposition steadily increased from the topmost layer (0–15 cm) to the deepest layer (45–60 cm), the latter exhibited the highest sulfide deposition (Table S2 and Figs. 6d, S2d). Similarly, all the enzyme activities studied displayed the highest activity in the topmost sub-soil layer (0–15 cm), with a decline in activity in the successively deeper layers (Table S3 and Figs. 7, S3). The sediment variables at all depths exhibited well distinguishable trends in sediment degradation across the various forest cover classes (high 60–100%; medium 30–60%; low 10–30%) (Figs. 5, 6, 7).

A pattern emerged when all measured parameters were plotted against the background of forest coverage in the 19 forests. For sand percentage and salinity, a general increasing trend in the values was observed with decreasing forest cover (Fig. 8a, d, respectively), whereas for clay, the percentage decreased with decreasing forest cover (Fig. 8c). The silt percentage seemed to remain unaffected by any change in forest cover (Fig. 8b). Ammonia-N, plant-available P, and SOC exhibited an overall decreasing tendency with a decline in forest coverage (Fig. 9c, a and b, respectively). However, sulfide accumulation generally exhibited a reversed (increasing) pattern with decreasing forest cover (Fig. 9d). The activities of all enzymes were also generally found to gradually decline with decreasing forest coverage (Fig. 10).

Pearson's correlation analysis was performed for the value of each sediment factor from different subsoil layers with the corresponding forest coverage. A

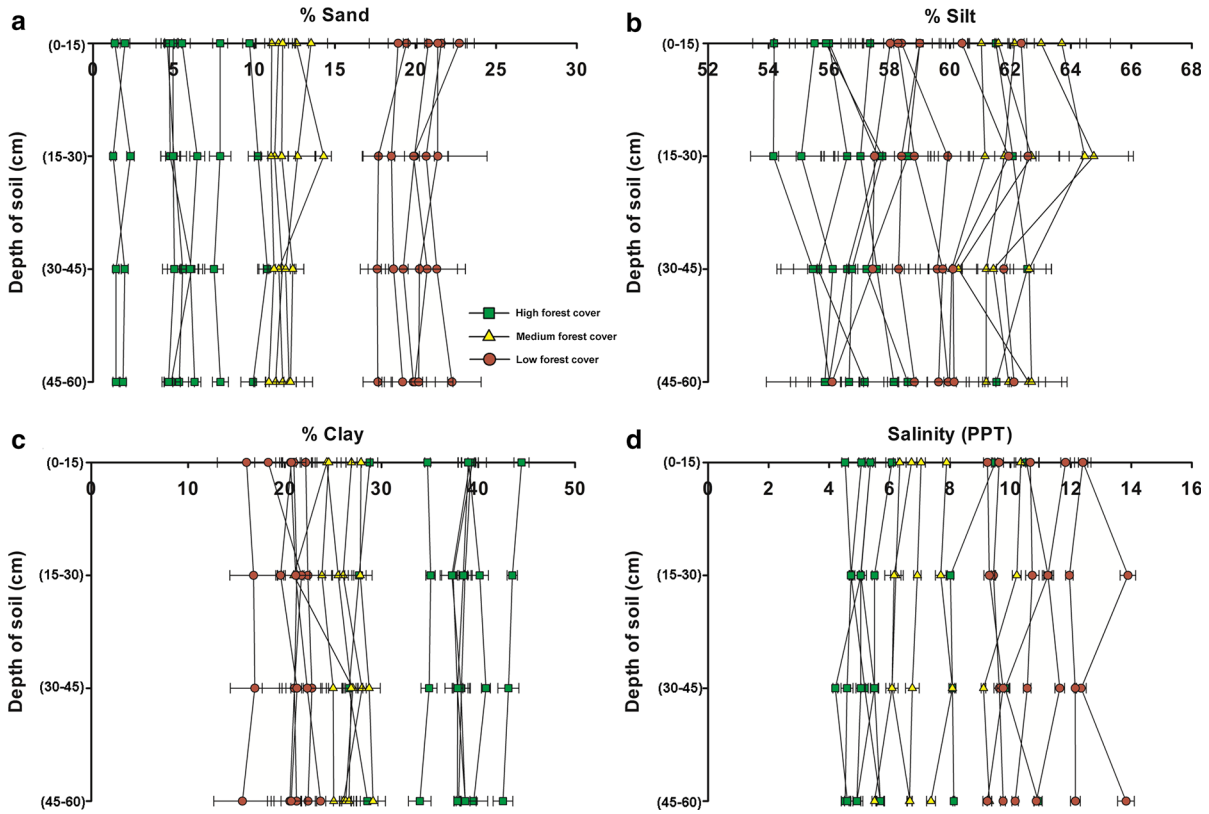

Fig. 5 Percentage of sand, silt, and clay along with sediment salinity across the 19 mangrove forests of Indian Sundarbans along different depths: **a** % of sand, **b** % of silt, **c** % of clay, and **d** sediment salinity. Forests have been grouped under three categories: high forest cover (60–100%), medium forest cover (30–60%) and low forest cover (10–30%). Here $n = 5$

strong and significant correlation was observed between each of the variables of each layer and forest cover, except for silt percentage (Table 1). With the exceptions of sand percentage, salinity, and sulfide, all sediment characters exhibited a positive correlation with forest cover, but sand, salinity and sulfide showed a negative correlation with forest coverage (Table 1).

A PCA was performed to reduce the dimensionality of the large datasets developed out of the sediment variables measured. In the plots, the variables are depicted as vectors and vector length indicates the significance of the parameter. Vector direction is indicative of the gradient of the variable in the ordination space (center to periphery). The length and direction of the vectors together describe the correlations of individual vectors with the axes (factor 1 and factor 2). In the PCA plot (Fig. 11), factor 1 (PC1) and factor 2 (PC2) were taken into consideration for the plot, as they together accounted for 78.348% of the cumulative variance in the dataset (Table S4). All enzyme activity measures, clay percentage, ammonia-N, plant-available phosphorus (P), and soil organic carbon (SOC) were grouped within the same cluster (PC1), whereas sulfide, salinity, pH, and sand percentage were clustered together (PC2) in the oppositely oriented direction (Fig. 11). The orientation of the two clusters in opposite directions in the plot (Fig. 11) indicated the strong negative correlation between the oppositely oriented groups of variables, which was already established from the patterns observed in Figs. 8, 9, and 10 and in our Pearson's correlation analysis (Table 1). We might conclude that forest cover is positively influenced by the activities of all the enzymes, clay, ammonia-N, plant-available phosphorus (P), and soil organic carbon (SOC) and negatively influenced by sulfide, salinity, pH, and sand. The vector for silt percentage was oriented far apart from these two clusters in a different quadrant, clearly

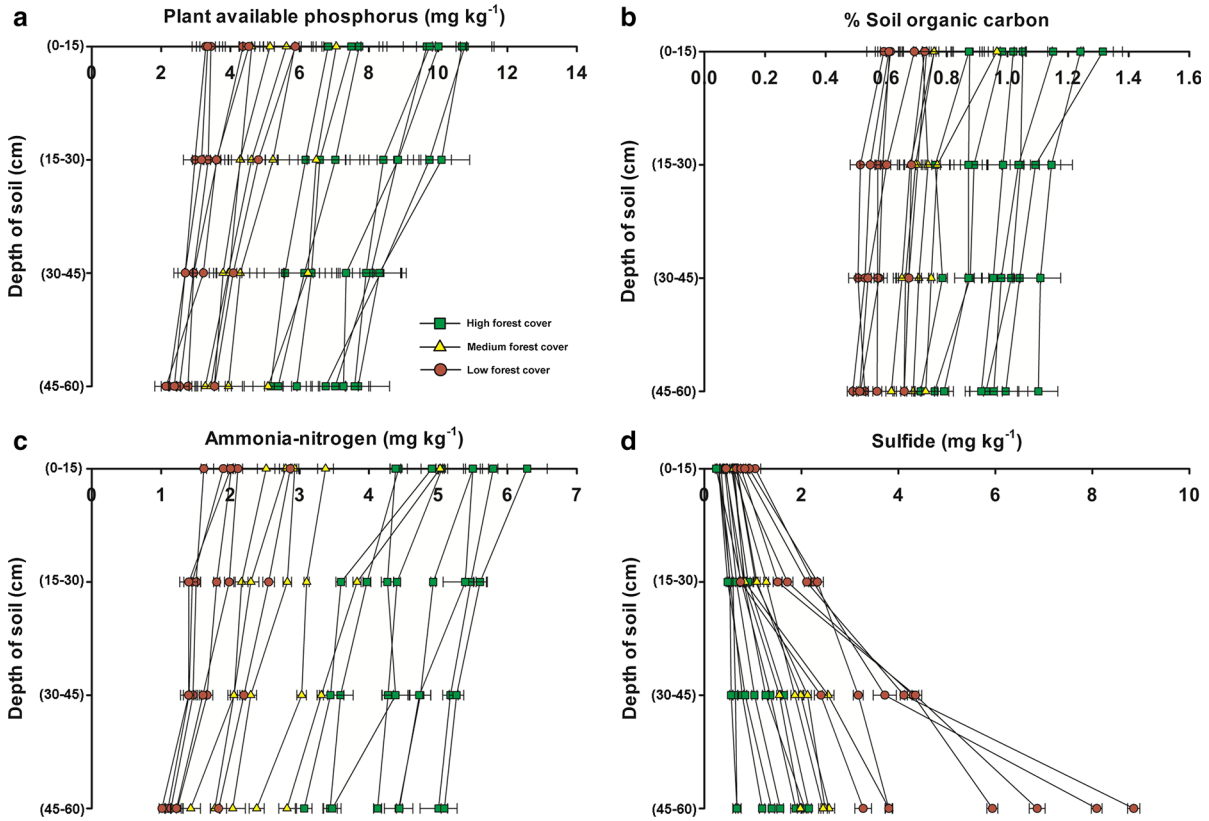

Fig. 6 Distribution of nutrients and sulfides in four sub-soils across the 19 mangrove forests of Indian Sundarbans: **a** plant-available phosphorus, **b** soil organic carbon, **c** ammonia-N, and **d** sulfide-sulfur. Forests have been grouped under three categories: high forest cover (60–100%), medium forest cover (30–60%) and low forest cover (10–30%). Here $n = 5$

establishing its independence and distinction with other sediment variables.

Mangrove forest structure analysis

In the forest structure analysis, we first analyzed the total forest coverage (percentage) for each of the 19 forests. The healthy undisturbed forests used as standard controls in this study (Bhagabatpur, Lakkhipur, Durbachoti, G-Plot and Lothian) possessed a range in forest cover between ∼ 85 and ∼ 98% (Fig. 12a). The other forests with moderate to severe degradation varied in forest coverage from ∼ 71 to ∼ 11% (Fig. 12a). Among the component species, we determined the coverage of 10 dominant species (*Avicennia alba* Blume, *Avicennia marina* (Forssk.) Vierh., *Avicennia officinalis* L., *Aegiceras corniculatum* (L.) Blanco, *Aegialitis rotundifolia* Roxb., *Phoenix paludosa* Roxb., *Heritiera fomes* Buch.-Ham., *Xylocarpus mekongensis* Pierre, *Excoecaria agallocha* L., and *Dalbergia spinosa* Roxb.) in each of the forests (Fig. 12a). Among the other less common species found in these forests were different species of *Ceriops*, *Bruguiera*, *Sonneratia*, and *Rhizophora,* which occur in small populations in some of the forests. When the DBH for each of these species was plotted (Fig. 12b), a clear reduction in DBH was observed for *Avicennia alba* and *Excoecaria agallocha* across healthy (control) to severely nutrient-limited forests. *Avicennia marina*, *Avicennia officinalis*, *Aegiceras corniculatum*, and *Aegialitis rotundifolia* also showed greatly reduced DBH in the exceedingly nutrient-poor forests of Rakkhoskhali, Dashpur 2, Ramganga, Atharogazi, Patharprotima, Gopalnagar, and Brajaballavpur (Fig. 12b). Accordingly, a similar pattern was observed for TBA, as TBA is dependent on the values of DBH. In terms of IVI, *Avicennia alba* possessed the highest IVI in Lakkhipur, whereas *Avicennia marina* exhibited a high IVI in many of the forests (Lakkhipur, Prentice, Lakkhipur

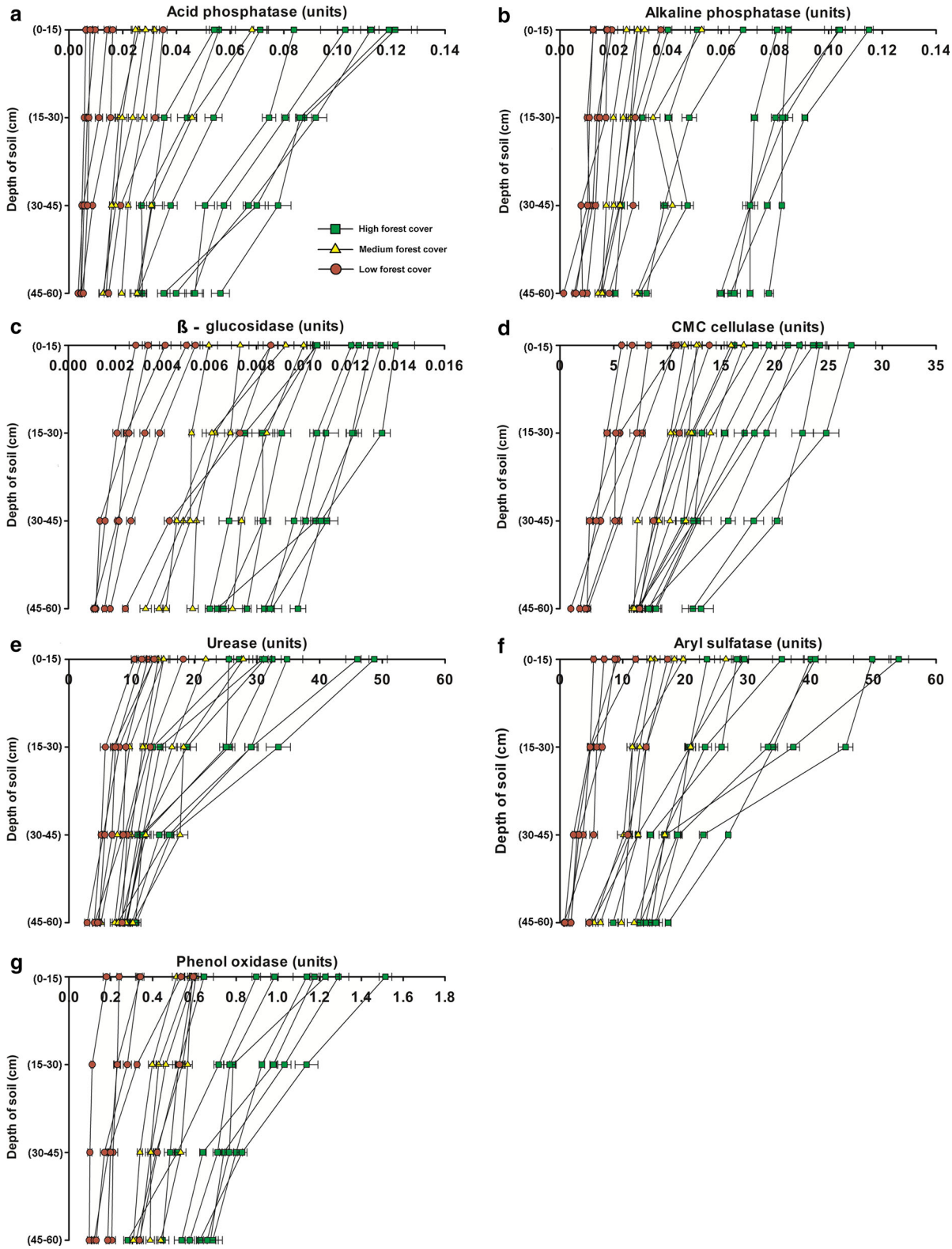
a
Acid phosphatase (units)
(0-15)
(15-30)
(30-45)
(45-60)
Depth of soil (cm)
0.00 0.02 0.04 0.06 0.08 0.10 0.12 0.14
High forest cover
Medium forest cover
Low forest cover
b
Alkaline phosphatase (units)
0.00 0.02 0.04 0.06 0.08 0.10 0.12 0.14
c
ß - glucosidase (units)
0.000 0.002 0.004 0.006 0.008 0.010 0.012 0.014 0.016
d
CMC cellulase (units)
0 5 10 15 20 25 30 35
e
Urease (units)
0 10 20 30 40 50 60
f
Aryl sulfatase (units)
0 10 20 30 40 50 60
g
Phenol oxidase (units)
0 0.2 0.4 0.6 0.8 1.0 1.2 1.4 1.6 1.8

◀**Fig. 7** Activity of microbial enzymes in four sub-soils across the 19 mangrove forests of Indian Sundarbans: **a** acid phosphatase, **b** alkaline phosphatase, **c** β-glucosidase, **d** CMC-cellulase, **e** arylsulfatase, **f** urease, and **g** phenol oxidase. Forests have been grouped under three categories: high forest cover (60–100%), medium forest cover (30–60%) and low forest cover (10–30%). Here $n = 5$. The units are a measure of enzyme activity and have been defined for each enzyme in materials and methods section

island, Dashpur 2, Ramganga, Patharprotima, Gopalnagar, and Brajaballavpur), proving itself as the species with the widest abundance (Fig. 12c). *Excoecaria agallocha* exhibited the highest IVI in Island X. *Heritiera fomes* had a small IVI and was present only in five forests. *Phoenix paludosa* had moderate to low IVI values and was also only present in five forests. *Xylocarpus mekongensis* had moderate to low IVI values and was detected in six forests. *Aegiceras corniculatum* and *Aegialitis rotundifolia* exhibited a wide range of IVI values and were observed in all forests (Fig. 12c). The IVI distribution of species seemed to be independent of nutritional control, and species appeared to have high IVI values even in greatly nutrient-limited forests.

Relative occurrence of mangrove species across the salinity gradient

When the species' relative occurrence scores were plotted against the corresponding habitat salinity, and combined on the same graphical plot to illustrate the relationship between the relative occurrence of species and habitat salinity, varying scenarios among mangrove forests were observed. The general pattern detected was that with declining forest cover, overall sediment salinity increased from the river's edge towards the landward side, and the relative occurrence of certain mangrove species changed concurrently (Tables 2, 3). In addition, decreases in the species'

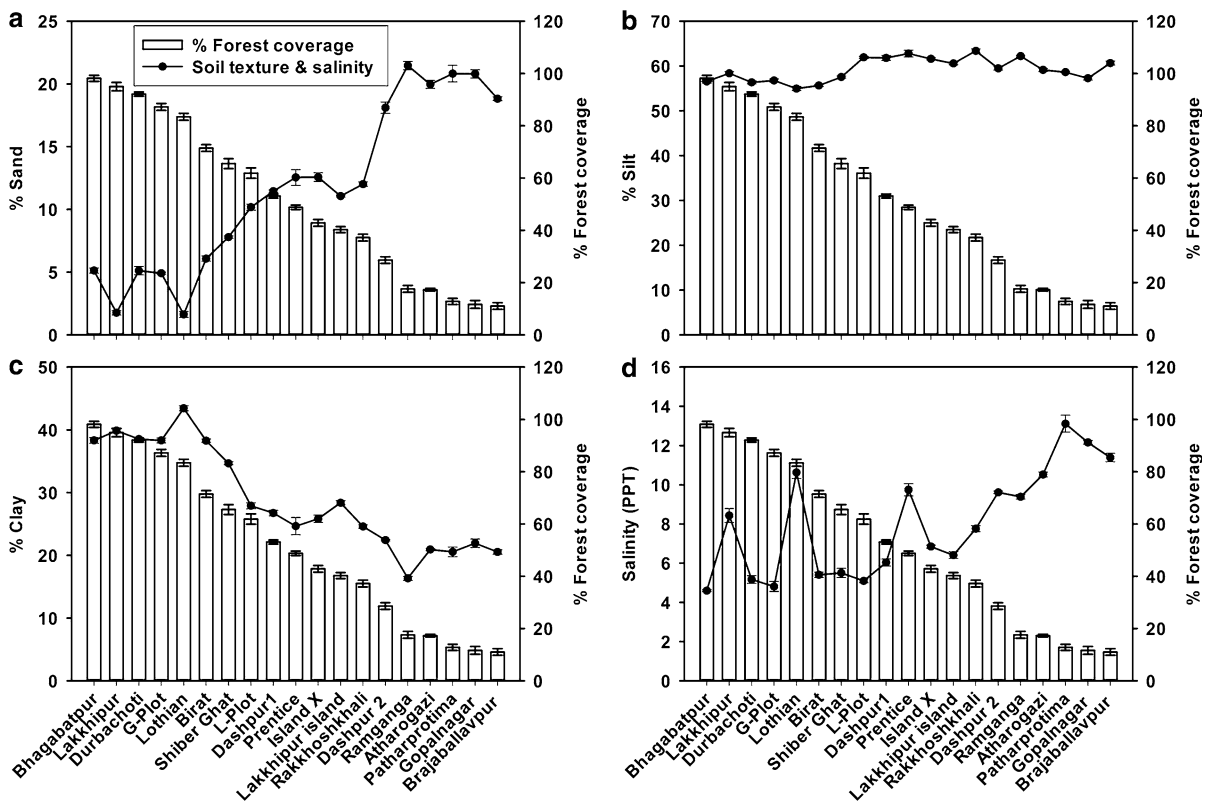

Fig. 8 Sand, silt, and clay percentages and salinity across the 19 mangrove forests of Indian Sundarbans against corresponding total forest coverage. The values of sediment variables plotted are an average of four sub-soils with standard error: **a** % of sand, **b** % of silt, **c** % of clay, and **d** sediment salinity. Here $n = 5$

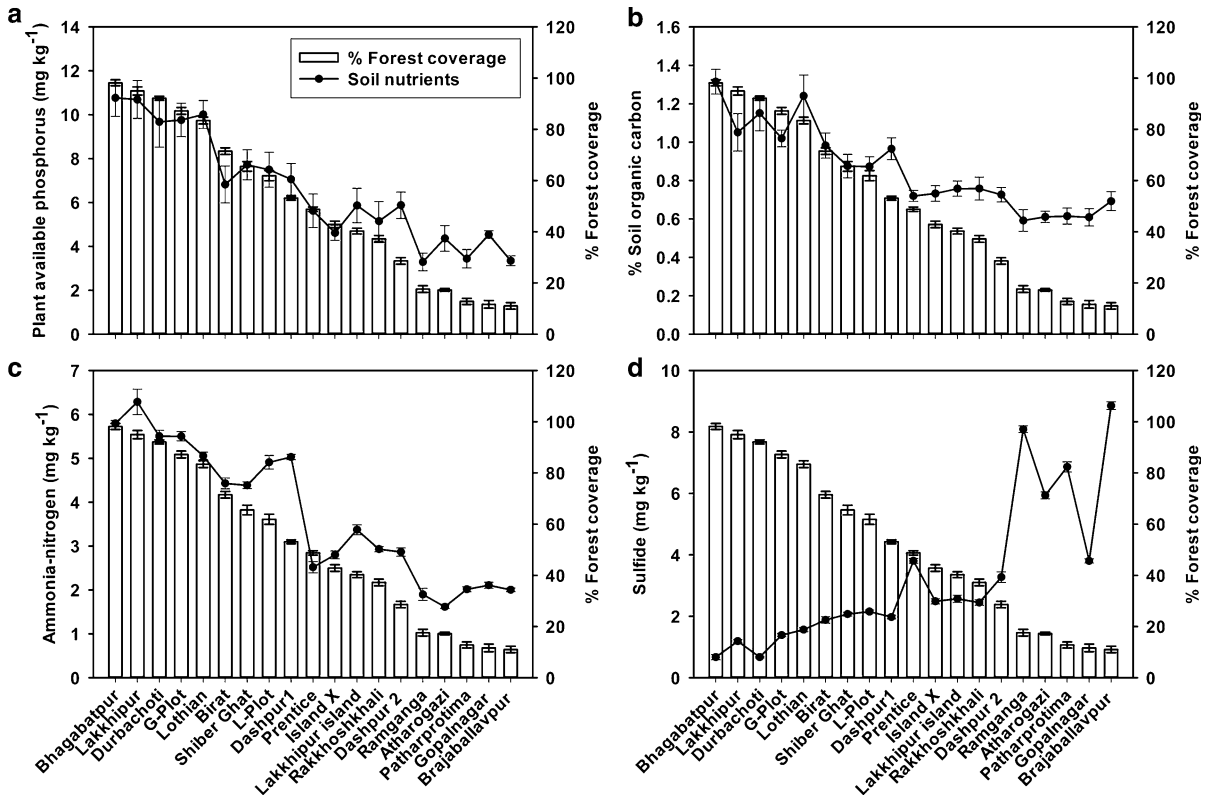

Fig. 9 Soil nutrients and sulfides across the 19 mangrove forests of Indian Sundarbans against corresponding total forest coverage. The values of **a** plant-available P, **b** soil organic carbon (SOC), and **c** ammonia-N plotted are the highest values observed in the topmost sub-soil (0–15 cm) with standard error. The **d** sulfide values are the amounts deposited in the deepest layer (45–60 cm) with standard error. Here $n = 5$

distance from the shoreline across forests were observed which could be expressed as apparent gradual advancement of mangroves towards the river's edge (Fig. 13 and Table 2), most likely due to incessant shoreline erosion. The advancement of the species towards the shoreline was understandable only on the basis of the decrease in respective scores of relative occurrence for each species observed in the different forests (Table 2). The relative position of each species and the corresponding habitat salinity were represented under four mangrove forests: Bhagabatpur (forest coverage ~ 98%, Fig. 13a), Dashpur 1 (forest coverage ~ 52%, Fig. 13b), Prentice (forest coverage ~ 49%, Fig. 13c), and Ramganga (forest coverage ~ 17%, Fig. 13d). For three species of *Avicennia* (*A. alba*, *A. marina*, and *A. officinalis*), a steady increase in habitat salinity was observed with little change in the relative position of the species among the forests (Fig. 13 and Tables 2, 3). For *Aegialitis rotundifolia* and *Aegiceras corniculatum*, the relative occurrence decreased towards the shoreline, as evidenced from their respective scores with increasing habitat salinity (Fig. 13 and Tables 2, 3). *Xylocarpus mekongensis* also showed apparent advancement but was found to be absent in many forests, perhaps because the salinity of the habitat surpassed the maximum tolerance level for this species in those forests (Fig. 13d and Tables 2, 3). *Heritiera fomes* slightly declined in distance from shoreline across the forests, while its population was completely absent in most of the forests in which the prevailing salinity exceeded 5.9 ppt (Fig. 13c, d and Tables 2, 3). *Phoenix paludosa* was absent where salinity surpassed the 6.5 ppt level (Fig. 13c, d and Tables 2, 3). *Excoecaria agallocha* showed a radical shift in occurrence from the back mangrove position to the position immediately adjacent to the shoreline (Fig. 13 and Table 2) and was dominant within all the degraded forests at higher salinities (Fig. 13b–d and Table 3). Similarly, *Dalbergia spinosa* exhibited a

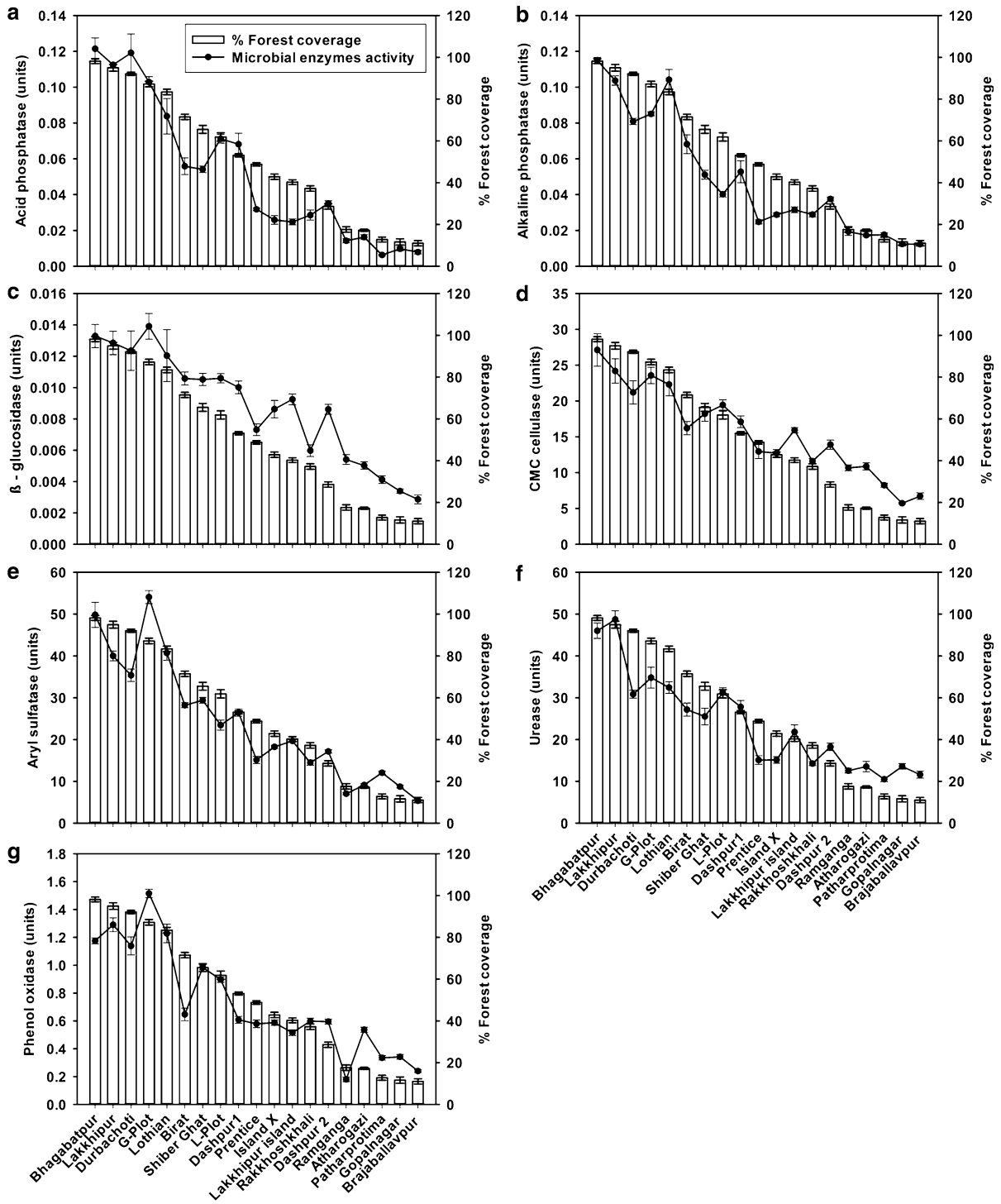

Fig. 10 Activity of microbial enzymes across the 19 mangrove forests of Indian Sundarbans against corresponding total forest coverage. The values of enzyme activities plotted are the highest values observed in the topmost sub-soil (0–15 cm) with standard error. Enzyme activity depicted include **a** acid phosphatase, **b** alkaline phosphatase, **c** β-glucosidase, **d** CMC-cellulase, **e** arylsulfatase, **f** urease, and **g** phenol oxidase. Here $n = 5$

Table 1 Pearson coefficients of correlation between each of the sediment variables at each of the sub-soils and % forest coverage across 19 mangrove forests of Indian Sundarbans

Soil variables	Forest coverage (%) of mangrove forests			
	Sub-soils			
	0–15 cm	15–30 cm	30–45 cm	45–60 cm
Acid phosphatase	0.932***	0.946***	0.661**	0.530**
Alkaline phosphatase	0.912***	0.936***	0.925***	0.466**
β-Glucosidase	0.935***	0.919**	0.957***	0.922***
CMC-cellulase	0.955***	0.949***	0.928***	0.900***
Urease	0.923***	0.849***	0.779**	0.786***
Arylsulfatase	0.932***	0.940***	0.929***	0.959***
Phenol oxidase	0.913***	0.933***	0.920***	0.860***
Plant-available phosphorus	0.960***	0.968***	0.966***	0.962***
Soil organic carbon	0.928***	0.963***	0.965***	0.937***
Ammonia nitrogen	0.948***	0.956**	0.967***	0.944***
Sulfide	− 0.863***	− 0.845***	− 0.926***	− 0.718***
% sand	− 0.922***	− 0.905***	− 0.899***	− 0.907***
% silt	− 0.335***	− 0.314***	− 0.364***	− 0.319***
% clay	0.819***	0.847***	0.871***	0.858***
Sediment pH	− 0.747***	− 0.768***	− 0.759***	− 0.785***
Sediment salinity	− 0.658***	− 0.675***	− 0.740***	− 0.655***

$^{*}P < 0.05$, $^{**}P < 0.01$, $^{***}P < 0.001$

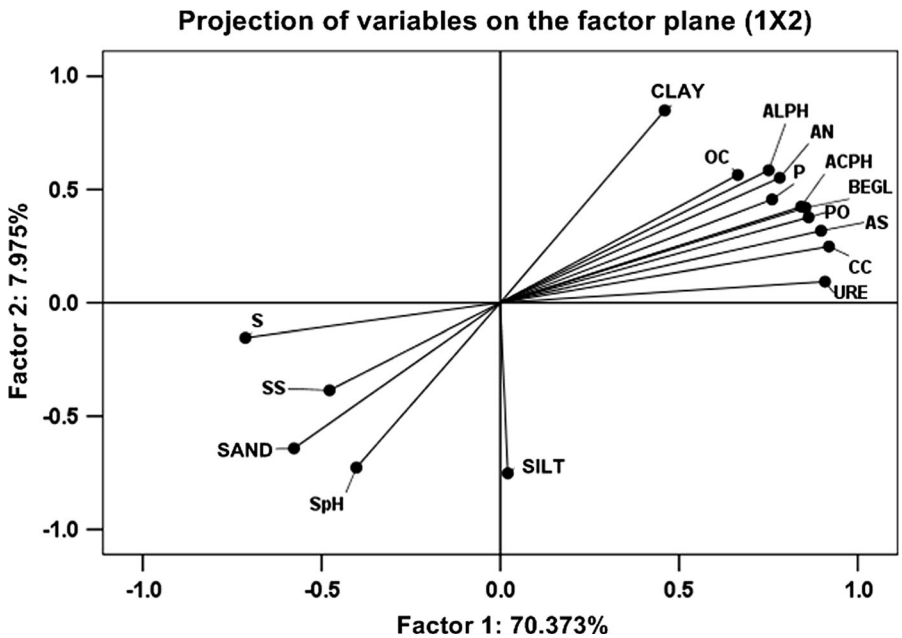

Fig. 11 Principal component analysis (PCA) of all the sediment variables examined: soil organic carbon (OC), alkaline phosphatase (ALPH), ammonia-N (AN), acid phosphatase (ACPH), plant-available phosphorus (P), β-glucosidase (BEGL), phenol oxidase (PO), arylsulfatase (AS), CMC-cellulase (CC), urease (URE), sulfide (S), sediment salinity (SS), and sediment pH (SpH)

drastic decrease in distance from shoreline, shifting its position from the landward side towards the position immediately adjacent to the shoreline (Fig. 13 and Table 2) with increased salinity (Table 3). All these findings indicate an overall decrease in species' distance from the shoreline (i.e., apparent gradual advancement of species' relative occurrence towards the shoreline across the healthy forests to more degraded forests concurrent with increases in habitat salinity) (Fig. 13 and Tables 2, 3).

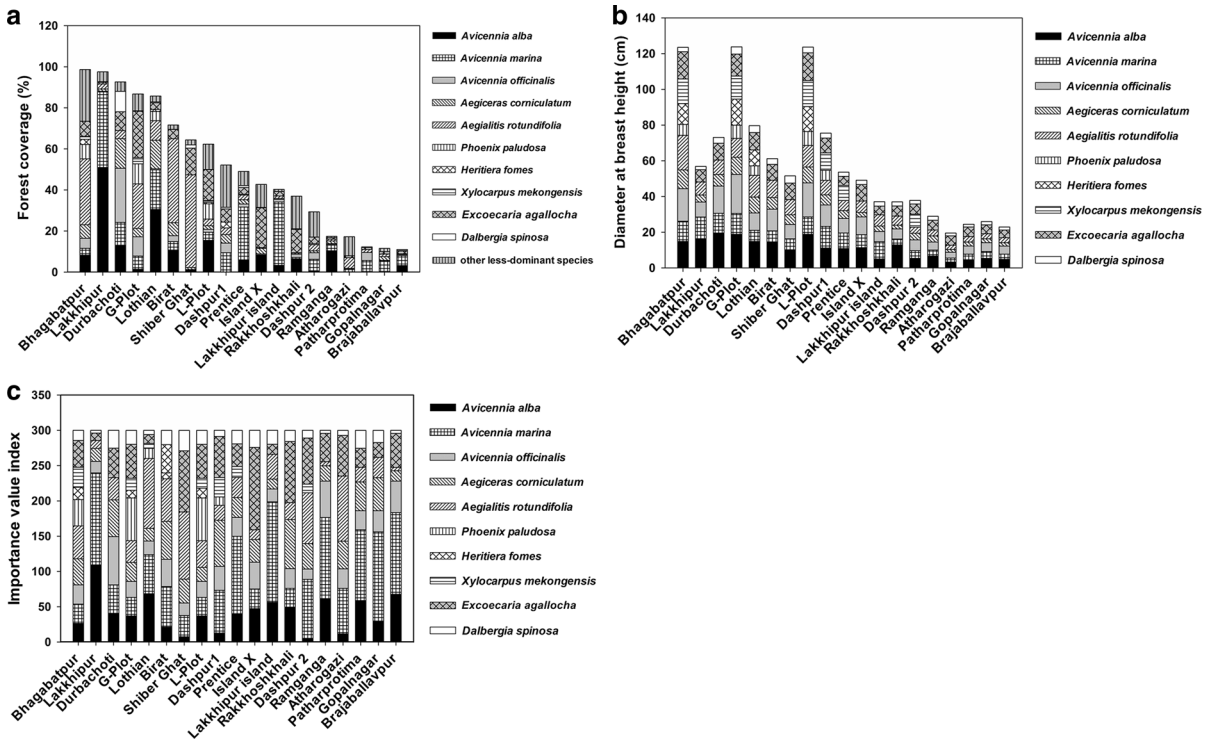

Fig. 12 Forest structure analyses of 19 forests in Indian Sundarbans: **a** total forest coverage with coverage for constituent species, **b** diameter at breast height (DBH), and **c** Importance Value Index (IVI)

Discussion

Nutrients as factors limiting forest coverage

The fringing mangrove forests of Sundarbans are facing degradation threats due to anthropogenic and natural stressors. In this study, we evaluated these affected forests in terms of the physical and chemical sediment properties and the structure and coverage of the forests in comparison to those of some neighboring healthy undisturbed mangrove forests. We attempted to correlate the observed nutrient limitation with the corresponding forest cover. We established that a gradual decline in forest cover was associated with a diminishing trend in nutrient content. All nutrient cycling enzymes (e.g., phosphatases which release soluble phosphorus; CMC-cellulases and β-glucosidases which decompose and release organic carbon; arylsulfatases which hydrolyze esters of sulfate to release sulfur; and ureases which hydrolyze peptides and urea), together facilitate the process of nutrient cycling in mangrove sediments. The activities of these enzymes may serve as indicators of soil nutrient availability (Cui et al., 2018). These enzymes were observed to exhibit higher activities in mangrove forests with higher forest coverage in our study. All these hydrolytic enzymes were found to be most active in the topmost sediment layer (0–15 cm), perhaps due to the higher availability of oxygen in this layer (Freeman et al., 2001).

Similarly, our study revealed that higher concentrations of plant-available P, ammonia-N, the most common and primary form of plant-available nitrogen in mangrove sediments (Twilley et al., 1986; Alongi, 1994; Kristensen et al., 2008), and soil organic carbon (SOC) were always associated with mangrove forests with higher forest cover. With a gradual reduction in these three nutrients from forest sediments, a concurrent decline in forest coverage was observed. Nutrient-limited sediments could be assumed to be one of the reasons for poor mangrove growth, among other stress factors. Interestingly, congruent to the pattern observed for the nutrient cycling enzyme activities, the highest concentrations of ammonia-N, P, and SOC were restricted to the topsoil (0–15 cm) in all 19

Table 2 Relative occurrence of 10 dominant species of mangroves across 19 forests of Indian Sundarbans

Name of the forests with % forest coverage	Relative occurrence of mangrove species denoted by scores across different forests									
	Avicennia alba	*Avicennia marina*	*Avicennia officinalis*	*Aegiceras corniculatum*	*Aegialitis rotundifolia*	*Phoenix paludosa*	*Heritiera fomes*	*Xylocarpus mekongensis*	*Excoecaria agallocha*	*Dalbergia spinosa*
Bhagabatpur (98.18)	0.40 ± 0.02	0.58 ± 0.03	0.60 ± 0.03	0.64 ± 0.03	0.59 ± 0.02	0.44 ± 0.02	0.97 ± 0.04	0.80 ± 0.04	0.95 ± 0.03	1.00 ± 0.05
Lakkhipur (94.99)	0.42 ± 0.03	0.48 ± 0.02	0.53 ± 0.02	0.62 ± 0.03	0.61 ± 0.04	–	–	–	0.94 ± 0.05	0.97 ± 0.05
Durbachoti (92.14)	0.41 ± 0.02	0.53 ± 0.02	0.57 ± 0.03	0.61 ± 0.04	0.55 ± 0.04	–	–	–	0.98 ± 0.05	0.99 ± 0.06
G-plot (87.21)	0.44 ± 0.03	0.52 ± 0.02	0.58 ± 0.02	0.65 ± 0.03	0.53 ± 0.04	0.49 ± 0.02	0.92 ± 0.05	0.83 ± 0.04	0.87 ± 0.05	0.94 ± 0.06
Lothian (83.42)	0.43 ± 0.04	0.51 ± 0.03	0.59 ± 0.03	0.64 ± 0.04	0.53 ± 0.03	0.51 ± 0.03	0.89 ± 0.05	–	0.85 ± 0.05	0.90 ± 0.04
Birat (71.51)	0.39 ± 0.03	0.53 ± 0.03	0.56 ± 0.04	0.58 ± 0.03	0.42 ± 0.02	–	–	–	0.65 ± 0.03	0.78 ± 0.05
Shiberghat (65.52)	0.40 ± 0.02	0.49 ± 0.03	0.54 ± 0.03	0.53 ± 0.03	0.48 ± 0.02	–	–	–	0.67 ± 0.05	0.81 ± 0.06
L-plot (61.91)	0.40 ± 0.04	0.51 ± 0.03	0.54 ± 0.02	0.58 ± 0.03	0.49 ± 0.04	0.43 ± 0.03	0.81 ± 0.04	0.72 ± 0.05	0.65 ± 0.05	0.83 ± 0.06
Dashpur 1 (53.14)	0.38 ± 0.02	0.57 ± 0.03	0.56 ± 0.04	0.56 ± 0.04	0.49 ± 0.02	0.35 ± 0.02	0.81 ± 0.04	0.78 ± 0.04	0.64 ± 0.05	0.72 ± 0.05
Prentice (48.77)	0.30 ± 0.02	0.40 ± 0.02	0.42 ± 0.03	0.50 ± 0.04	0.32 ± 0.02	–	–	0.58 ± 0.03	0.50 ± 0.03	0.51 ± 0.04
Island X (42.84)	0.32 ± 0.01	0.44 ± 0.03	0.43 ± 0.04	0.51 ± 0.03	0.35 ± 0.04	–	–	–	0.52 ± 0.04	0.54 ± 0.03
Lakkhipur island (40.25)	0.30 ± 0.02	0.41 ± 0.03	0.44 ± 0.04	0.53 ± 0.04	0.34 ± 0.02	–	–	–	0.52 ± 0.03	0.55 ± 0.03
Rakkhoskhali (37.21)	0.33 ± 0.01	0.42 ± 0.03	0.41 ± 0.03	0.51 ± 0.02	0.34 ± 0.03	–	–	–	0.50 ± 0.02	0.54 ± 0.04
Dashpur 2 (28.59)	0.30 ± 0.01	0.42 ± 0.02	0.44 ± 0.03	0.53 ± 0.03	0.43 ± 0.02	–	–	0.56 ± 0.03	0.51 ± 0.02	0.53 ± 0.02
Ramganga (17.61)	0.30 ± 0.01	0.40 ± 0.02	0.39 ± 0.03	0.49 ± 0.03	0.32 ± 0.02	–	–	–	0.38 ± 0.03	0.45 ± 0.03
Atharogaji (17.27)	0.33 ± 0.02	0.39 ± 0.03	0.40 ± 0.02	0.43 ± 0.02	0.36 ± 0.02	–	–	–	0.40 ± 0.03	0.43 ± 0.04
Patharpratima (12.79)	0.30 ± 0.02	0.38 ± 0.02	0.40 ± 0.03	0.42 ± 0.03	0.36 ± 0.01	–	–	–	0.39 ± 0.02	0.42 ± 0.02
Gopalnagar (11.64)	0.32 ± 0.01	0.37 ± 0.02	0.39 ± 0.02	0.40 ± 0.03	0.34 ± 0.04	–	–	–	0.40 ± 0.03	0.41 ± 0.03
Brajaballavpur (11.01)	0.33 ± 0.02	0.35 ± 0.03	0.36 ± 0.04	0.41 ± 0.03	0.35 ± 0.03	–	–	–	0.42 ± 0.02	0.44 ± 0.03

A gradual decrease in relative occurrence score is observed for most species moving from forests with high cover percentage (healthy undisturbed control forests) towards forests with low cover percentage (degraded forests). Decrease in relative occurrence score appears as mangrove species advance towards shoreline. The results are represented as averages with standard deviation and here $n = 5$

Table 3 Varying habitat salinity of ten dominant species of mangroves across 19 forests of Indian Sundarbans

Name of the forests with % forest coverage	Habitat salinity (in ppt) of mangrove species across different forests									
	Avicennia alba	*Avicennia marina*	*Avicennia officinalis*	*Aegiceras corniculatum*	*Aegialitis rotundifolia*	*Phoenix paludosa*	*Heritiera fomes*	*Xylocarpus mekongensis*	*Excoecaria agallocha*	*Dalbergia spinosa*
Bhagabatpur (98.18)	4.77 ± 0.13	4.50 ± 0.18	4.48 ± 0.11	4.40 ± 0.21	4.50 ± 0.18	4.72 ± 0.13	4.26 ± 0.22	4.30 ± 0.32	4.28 ± 0.21	4.25 ± 0.38
Lakkhipur (94.99)	9.55 ± 0.43	9.44 ± 0.45	8.98 ± 0.66	8.32 ± 0.21	8.32 ± 0.32	–	–	–	7.82 ± 0.32	7.69 ± 0.44
Durbachoti (92.14)	6.02 ± 0.43	5.88 ± 0.41	5.21 ± 0.22	4.88 ± 0.18	5.42 ± 0.23	–	–	–	4.72 ± 0.34	4.60 ± 0.42
G-plot (87.21)	5.23 ± 0.44	4.53 ± 0.17	4.40 ± 0.12	4.22 ± 0.19	4.51 ± 0.24	4.98 ± 0.21	3.94 ± 0.33	4.12 ± 0.35	3.98 ± 0.18	3.95 ± 0.11
Lothian (83.42)	11.76 ± 0.62	10.54 ± 0.54	10.12 ± 0.55	9.82 ± 0.21	10.22 ± 0.34	6.54 ± 0.31	5.66 ± 0.52	–	9.69 ± 0.32	9.51 ± 0.44
Birat (71.51)	6.02 ± 0.41	5.24 ± 0.35	5.13 ± 0.33	5.08 ± 0.29	5.62 ± 0.17	–	–	–	4.99 ± 0.21	4.92 ± 0.26
Shiberghat (65.52)	6.66 ± 0.54	5.83 ± 0.42	5.72 ± 0.44	5.78 ± 0.28	5.92 ± 0.21	–	–	–	5.37 ± 0.19	5.18 ± 0.17
L-plot (61.91)	5.56 ± 0.44	5.31 ± 0.41	5.02 ± 0.30	4.88 ± 0.42	5.44 ± 0.28	5.52 ± 0.31	4.51 ± 0.33	4.63 ± 0.42	4.74 ± 0.49	4.40 ± 0.19
Dashpur 1 (53.14)	6.02 ± 0.57	5.98 ± 0.48	5.98 ± 0.44	5.98 ± 0.62	6.02 ± 0.21	6.04 ± 0.22	5.94 ± 0.19	5.94 ± 0.17	5.95 ± 0.28	5.95 ± 0.31
Prentice (48.77)	7.79 ± 0.32	7.78 ± 0.34	7.76 ± 0.41	7.62 ± 0.22	7.79 ± 0.29	–	–	7.62 ± 0.19	7.68 ± 0.08	7.68 ± 0.16
Island X (42.84)	7.29 ± 0.41	6.57 ± 0.40	6.59 ± 0.17	6.42 ± 0.13	6.98 ± 0.32	–	–	–	6.33 ± 0.22	6.21 ± 0.16
Lakkhipur island (40.25)	6.95 ± 0.65	6.42 ± 0.18	6.33 ± 0.11	5.99 ± 0.44	6.79 ± 0.28	–	–	–	6.12 ± 0.53	5.89 ± 0.15
Rakkhoskhali (37.21)	8.40 ± 0.66	7.87 ± 0.37	7.89 ± 0.28	7.44 ± 0.12	8.20 ± 0.19	–	–	–	7.52 ± 0.44	7.31 ± 0.32
Dashpur 2 (28.59)	10.13 ± 0.19	10.07 ± 0.16	9.91 ± 0.27	9.57 ± 0.24	9.82 ± 0.32	–	–	7.31 ± 0.38	9.42 ± 0.52	9.33 ± 0.40
Ramganga (17.61)	11.52 ± 0.18	11.40 ± 0.30	11.40 ± 0.22	11.32 ± 0.42	11.52 ± 0.18	–	–	–	11.52 ± 0.21	11.32 ± 0.32
Atharogaji (17.27)	11.35 ± 0.66	10.52 ± 0.54	9.99 ± 0.12	9.78 ± 0.18	10.87 ± 0.45	–	–	–	9.99 ± 0.32	9.78 ± 0.19
Patharpratima (12.79)	14.02 ± 0.44	13.09 ± 0.38	12.35 ± 0.52	11.89 ± 0.21	13.42 ± 0.33	–	–	–	13.09 ± 0.45	11.89 ± 0.34
Gopalnagar (11.64)	12.28 ± 0.21	11.92 ± 0.19	11.83 ± 0.33	11.72 ± 0.43	12.03 ± 0.21	–	–	–	11.72 ± 0.31	11.65 ± 0.33
Brajaballavpur (11.01)	12.01 ± 0.42	11.41 ± 0.64	11.32 ± 0.37	10.99 ± 0.12	11.41 ± 0.28	–	–	–	10.82 ± 0.43	10.66 ± 0.35

A gradual increase in salinity of the habitat is observed for most species moving from forests with high cover percentage (healthy undisturbed control forests) towards forests with low cover percentage (degraded forests). Some of the species were well acclimated with the increased habitat salinity, whereas *Phoenix paludosa*, *Heritiera fomes*, *Xylocarpus mekongensis* were absent in many forests. The results are represented as averages with standard deviation and here $n = 5$

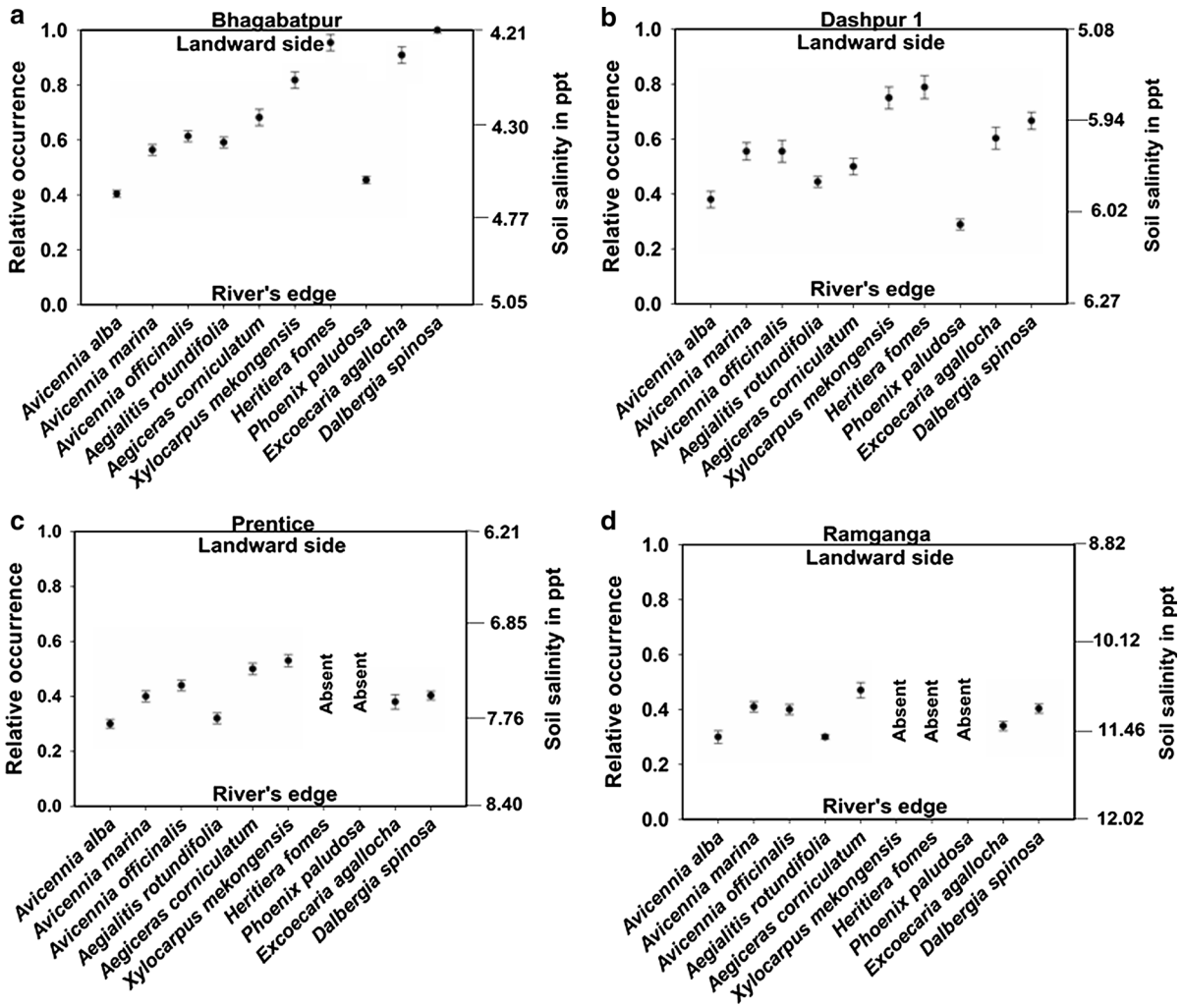

Fig. 13 Graphical representation of the species' relative occurrence against salinity gradient as observed in representative mangrove forests of varying degradation status from river's edge towards the furthest inland: **a** Bhagabatpur (∼ 98.6% forest coverage), **b** Dashpur 1 (∼ 52.4% forest coverage), **c** Prentice (∼ 49% forest coverage), and **d** Ramganga (∼ 17% forest coverage)

forests with progressively reduced availability at greater depths.

We failed to find any significant differences in nutrient content or enzyme activity in the mangrove sediments across the dry and wet seasons (Supplementary Files 2 and 3), although variations were observed with depth. It became obvious that the maximum nutrient availability always remained confined to the topmost sediments in the mangrove forests. In a study of Peninsular Malaysian mangrove forests (Sofawi et al., 2017), sediment carbon, nitrogen, phosphorus, and potassium were also found to differ significantly across locations but not between seasons. With the exception of phosphorus in one forest, depth did not influence the nutrient availability in mangrove sediments in their study. A similar study (Dinesh et al., 2004) was conducted on sediments associated with undisturbed and disturbed mangroves in South Andaman, India. Dinesh et al. (2004) results were quite similar to our findings. The activities of extracellular hydrolytic enzymes that were involved in carbon, nitrogen, sulfur, and phosphorus cycling in mangrove sediments (e.g., phosphomonoesterase, phosphodiesterase, β-glucosidase, urease, BAA-protease, casein-protease, arylsulfatase, invertase, and carboxymethylcellulase), were found to show drastic

reductions in activities in disturbed sites in comparison to undisturbed sites. Similarly like our observations, the organic carbon, total nitrogen, soluble phosphorus, and potassium levels were considerably lower at disturbed sites, with distinct reductions in microbial biomass and activity. Thus, the biochemical properties of soil can be very sensitive to environmental stress and provide rapid and accurate estimates of changes in the quality of sediments subjected to degradation (Dinesh et al., 2004). These studies on sediment quality of mangrove forests are of immense importance in the development of soil management strategies within degraded mangrove forests.

The movement of nutrients through mangrove ecosystems is an elusive aspect of the function of these ecosystems (Lugo, 1999). Nutrient availability was found not to be uniform within mangrove forests and could switch from N to P limitation across narrow environmental gradients (Boto & Wellington, 1983; McKee, 1993). Temperate coastal ecosystems have been reported to be nitrogen (N) limited (Valiela & Teal, 1979), but the few tropical and subtropical mangrove wetlands that had been studied appeared to be primarily phosphorus (P) limited (Boto & Wellington, 1983; Feller, 1995; Feller et al., 1999). Phosphorus deficiency was shown to be a major factor limiting plant growth in dwarf mangrove forests (Feller, 1995). The lower relative availability of P per unit of N indicated that P was a limiting nutrient for mangroves in the oligohaline zone of the Shark River estuary (Chen & Twilley, 1999). It was also proposed that N and P limit mangrove growth in approximately equal proportions (Elser & Hamilton, 2007). Our analyses also unequivocally established ammonia-N and plant-available P as two indispensable nutrients limiting mangrove forest coverage.

Anoxicity, sediment texture and salinity control over forest structure

The accumulation of phenolic compounds in soil can directly inhibit microbial biodegradation because the enzyme phenol oxidase which degrades phenolics is known to be inhibited by these phenolic compounds (Kirwan & Megonigal, 2013). Findings of other studies have supported the idea that oxygen constraints on a single enzyme, phenol oxidase can minimize the activity of hydrolytic enzymes responsible for decomposition (Freeman et al., 2001). The higher activity of phenol oxidase enzyme ensures less oxygen constraints and allows subsequent unhindered microbial decomposition by microbe-secreted pivotal hydrolytic enzymes. In this study, the higher activity of phenol oxidase being linked to healthy (control) mangrove forests and the gradual decline of the activity of this enzyme in more disturbed mangrove sediments indicated a prevalence of hindered nutrient cycling and higher anoxicity in degraded mangrove sediments.

Apart from this, in the anoxic mangrove niche, sulfate reduction is the dominant pathway for organic matter respiration by sulfate reducing bacteria (SRB), resulting in the accumulation of sulfides that are toxic to mangroves (Reef et al., 2010). As SRBs prefer to exist in anaerobic conditions, sulfides are deposited within deeper sediments. Our study also revealed that the greatest deposition of sulfides occurred in the deepest layer (45–60 cm). Relatively high sulfide accumulation was observed across the more degraded forests. We presume the prevalence of higher anoxic condition across more degraded mangroves has caused this higher build-up of sulfides. Our analyses clearly established sulfide deposition as an important stressor negatively controlling mangrove forest cover.

In the sediment texture analysis, three different patterns emerged for the three soil components: sand, clay and silt. An increase in sand percentage and a decrease in clay percentage in the sediments were associated with reduced forest cover, while the silt percentage remained generally the same across all the forests. This established a strong negative correlation for sand, a positive association for clay, and a neutral relationship for silt with respect to forest cover.

In addition, we found that salinity negatively affected the mangrove forest cover. Decreases in vegetation growth due to salt toxicity and detrimental osmotic potential result in lower carbon (C) inputs into the soil and the further deterioration of its physical and chemical properties (Wong et al., 2009). Soil enzyme activities have also been reported to decrease with increasing levels of salinity (Batra & Manna, 1997). Hypersalinity prevailed in the more disturbed mangrove forests, adversely affecting their growth and abundance, as observed in our study.

Changes in mangrove forest structure with the gradual depletion of nutrients

Variation in forest structure appears closely related to soil fertility (Reise et al., 2010). Nutrients have been identified as determinants of mangrove structural development, but most investigations carried out in mangrove forests were based on the availability of the two macronutrients phosphorus (P) and nitrogen (N). Cruz et al. (2013) observed that the inundation frequency, availability of P in the sediments, P in the leaves, and interstitial salinity were the primary factors determining the distribution of *Avicennia germinans* and *Rhizophora mangle* on the Bragança Peninsula in northern Brazil. The landward decline of mangrove basal area and biomass was found to be associated with a decrease in total P with more constant total N concentrations (Chen & Twilley, 1999). In association with the gradual general decline of ammonia-N, plant-available P, organic carbon, and related enzyme activities across the 19 forests in our study, a steady decline was also reflected in total forest cover and in the DBH of three species of *Avicennia*, *Excoecaria agallocha*, *Aegialitis rotundifolia*, and *Aegiceras corniculatum*. A similar decline in TBA in these species was observed across the progressive nutrient depletion in affected forests. Interestingly, nutrient depletion did not influence the IVI of the mangrove species. The IVI of the species remained unaffected by nutrient deficiency, and even high IVI values were recorded for different species from extremely nutrient-limited forests.

Varying habitat salinity and its effect on mangrove occurrence and zonation

Mangrove species zonation was reported to occur at a macro scale across the entire delta of Sundarbans along a northeast–southwest salinity gradient (Curtis, 1933; Choudhury, 1968). Along the east coast of Africa, the coastal mangrove forests of Tanzania were also reported to exhibit zonation (Walter, 1971). Similar zonation and species distribution for Sundarban mangroves were reported by Joshi & Ghose (2003), in which mangrove distribution was related to sediment salinity and pH gradients. *Acanthus ilicifolius* L., *Avicennia alba*, and *Avicennia marina* were reported to dominate sites with high salinity due to regular diurnal tidal inundation, while *Aegiceras corniculatum, Ceriops decandra* (Griff.) Ding Hou, *Dalbergia spinosa, Derris trifoliata* Lour., and *Excoecaria agallocha* were found to be restricted to low-salinity areas (Joshi & Ghose, 2003).

In our study, when the relative occurrence of mangroves was graphically represented across the salinity gradient, a clear steady increase in the native habitat salinity of many mangrove species was observed from the rivers' edge towards inland areas in more degraded mangrove forests (Fig. 13b–d). A gradual increase in sediment salinity prevails, which is dependent on intrusive tidal inundation caused by gradual shoreline erosion. As observed in our studied forests, all mangrove species generally appeared to be advancing towards the shoreline based on the observed decrease in their distance from shoreline and also decreases in their respective scores of relative occurrence (Table 2). Even mangroves, such as *Excoecaria agallocha* and *Heritiera fomes* that are known to colonize only the lower salinity zones as back mangrove species in healthy forests (Joshi & Ghose, 2003; Sarker et al., 2016) were found to be shifting towards higher-salinity habitats, as observed in this study (Table 3). This net alteration in habitat salinity is likely to cause instability in mangrove growth and expansion. *Excoecaria agallocha* was found to adjust to this rise in habitat salinity and was abundant in all 19 mangrove forests (Table 3), while *Heritiera fomes* failed to expand as the increases in salinity exceeded the tolerance limit for this species (Fig. 12a). In the present circumstances, *E. agallocha* can no longer be considered a back mangrove which is evident from its scores of relative occurrence found in degraded forests of Indian Sundarbans (Table 2). *Heritiera fomes* prefers low salinity (Sarker et al., 2016) and is sensitive to this steady rise in habitat salinity. This species is now absent in many mangrove forests of Indian Sundarbans, as supported by the species composition of our studied forests (Figs. 12, 13c, d). Sarker et al. (2016) reported *Heritiera fomes* to be on the verge of extinction in Indian Sundarbans as a result of increased salinity. In Bangladesh Sundarbans, *H. fomes* abundance usually decreased with increasing habitat salinity (> 7 dS m^{-1}) (Sarker et al., 2016). A contrasting situation exists with *Excoecaria agallocha* in which *E. agallocha* habitat maps indicate its wide distribution across the entire Sundarbans of Bangladesh due to its high salt tolerance and ability to quickly expand in open and degraded mangrove habitats

(Sarker et al., 2016). Furthermore, high salinity levels are the likely reason for the absence of *Phoenix paludosa* and *Xylocarpus mekongensis* from many forests because of the measured high salinity levels in the soil cores and the known sensitivity of these species to high salinity (Payo et al., 2016; Fig. 13c, d). The three species of *Avicennia* were observed to flourish like *E. agallocha* irrespective of the rising salinity, proving their tolerance to a wide range of salinities (Joshi & Ghose, 2003). Landward sediment salinity was observed to be higher (Fig. 13) in highly degraded forests, and the salinity-dependent zonation of mangroves remained unperturbed in the healthy undisturbed (control) mangrove forests in Indian Sundarbans (Fig. 13a and Table 3).

Potential of sea level rise to affect species distributions in Indian Sundarbans

Sea level rise (SLR) has been projected to be a major threat to mangrove ecosystems associated with climate change (Ward et al., 2016). Mangroves are very susceptible to changes in flooding duration and the frequency of tidal surges resulting in salinity rise because they possess species-specific physiological thresholds of salinity tolerance (Ball, 1988; Friess et al., 2012). Increases in the inundation period can lead to shifts in species composition (Gilman et al., 2008). A recent global meta-analysis established that back mangroves are less vulnerable to sea level rise than fringing mangrove types due to species and sediment deposition differences (Ward et al., 2016). The high species diversity of South East Asia's mangrove communities likely makes them more resilient to SLR (Ward et al., 2016) as multispecies forests are more resilient to SLR due to interspecific facilitation (Huxham et al., 2010) and increased below-ground root production (Lang'at et al., 2014), allowing mangroves to increase their surface elevation through biogenic processes. Coastal wetlands may transition from salt marsh to mangrove-dominated zones as an effect of SLR, as mangroves exhibit greater rates of surface elevation change compared to salt marshes, better enabling mangroves to keep pace with SLR (Ward et al., 2016). The Sundarban mangrove ecosystem has also become a victim of SLR not only because of the observed submergence of low-lying islands (Center for Science and Environment, India, 2012) but also because the species composition is expected to be greatly affected. Payo et al. (2016) clearly cited that SLR will lead to a decreased distribution of some dominant freshwater-loving species assemblages (e.g., *Heritiera fomes*, *Ceriops* spp., and *Xylocarpus* spp.) with a concomitant increase in more salt-tolerant species (e.g., *Excoecaria agallocha*, *Sonneratia* spp., and *Bruguiera* spp.) among the Sundarban mangroves. Our observations from this study, although not based on data collected across different time periods, demonstrated an increase in salinity across different mangrove forests in Indian Sundarbans. Assuming that this salinity increase has resulted from the reduction in freshwater discharge from the Ganges River, as well as SLR, we opine that SLR has great potential to change the species composition. Our observation that salt-sensitive *Heritiera fomes*, *Xylocarpus* spp., and *Phoenix paludosa* were absent from most of the studied forests and that salt-tolerant *Excoecaria agallocha* and *Avicennia* spp. were expanding in and dominating all the studied mangrove forests might be cited as an example of the possible influence of SLR on mangrove species distributions in Indian Sundarbans.

Conclusion

Based on the study results described here, apparent relationships between the studied sediment factors and corresponding forest cover were clearly established. Mangroves' natural adaptations to high salinity and low nutrients can be defended against our observed consequences of habitat degradation. The observed nutrient reduction and increases in salinity, sulfide, and sand percentage, the major negative controlling factors influencing mangrove forest cover, were strongly correlated with decline in forest coverage from $\sim$ 98 to $\sim$ 11%, which could not be a mere coincidence. Unlike healthy forests, degraded forests exhibited visible degradation in terms of forest clearing, poor stunted growth of vegetation, and dominance of monotypic salt-tolerant species caused by anthropogenic and natural stressors. Our statistical analyses strengthened the hypothesis that forest cover can be positively or negatively influenced by various sediment characteristics. Had the nutrient limitation and salinity increases developed gradually and naturally, the forest cover and structure would not have been affected so greatly, a strong statistical

relationship would have been lacking, and the mangroves would have developed resilience to face these natural limitations.

Our transect study strongly establishes salinity intrusion as a primary mechanism for forest degradation. Controlled and maintained by tidal flushes, salinity decreases from the river's edge toward landward side. Our study reveals as these systems move from healthy to more degraded forests, within hundred meters from shoreline towards inland, the sediment salinity increases on both sides, riverward as well as landward side (Table 3). In healthy forests, salinity-sensitive species are growing towards landward side, while high salinity tolerant species are growing towards the river's edge (Table 2 and Fig. 13a). Contrastingly, in more degraded forests this salinity restricted zonation of mangroves is observed to be disrupted. Species are rather crowded within a short salinity stretch, though on higher range, more toward the river's edge (Fig. 13b–d). Some species that are more intolerant of higher salinity levels are absent from many forests. At present, *Heritiera fomes*, which has a restricted distribution in India and Bangladesh, is declared endangered, and *Phoenix paludosa* is considered near threatened by the International Union for Conservation of Nature (IUCN). *Excoecaria agallocha* is the only exceptional species that not only adjusts to salinity rise but can also expand its distribution from low-salinity to higher-salinity habitats, as observed in this study.

Acknowledgements We gratefully acknowledge the financial support by Department of Biotechnology, Government of India for carrying out the research work (File No. BT/PR7501/BCE/8/982/2013). We sincerely acknowledge the permission granted by Sundarban Biosphere Reserve, West Bengal, India to carry out the survey across the mangroves of Indian Sundarbans. Help rendered by all our field assistants during the field work, especially by Mr. Ranjan Pradhan, is also thankfully acknowledged. The helping hand offered in making the GIS maps by Ms. Radhika Bhargava, Department of Geography, National University of Singapore is also gratefully acknowledged. Our sincere thanks go to Michael J. Baldwin of U.S. Geological Survey and Dr. Ramanuj Konar of Sarat Centenary College for carefully reading the manuscript and their suggested changes that helped to improve the manuscript. The authors would like to express their sincere thanks to the associate editor Dr. K. W. Krauss and all the three anonymous reviewers for their valuable comments and critical suggestions made on earlier versions of the manuscript which helped us to improve it.

References

Alongi, D. M., 1994. The role of bacteria in nutrient recycling in tropical mangrove and other coastal benthic ecosystems. Hydrobiologia 285: 19–32.

Alongi, D. M., 2010. Dissolved iron supply limits early growth of estuarine mangroves. Ecology 91: 3229–3241.

Bach, C. E., D. D. Warnock, D. J. Van Horn, M. N. Weintraub, R. L. Sinsabaugh, S. D. Allison & D. P. German, 2013. Measuring phenol oxidase and peroxidase activities with pyrogallol, L-DOPA, and ABTS: effect of assay conditions and soil type. Soil Biology & Biochemistry 67: 183–191.

Ball, M. C., 1988. Ecophysiology of mangroves. Trees 2: 129–142.

Batra, L. & M. C. Manna, 1997. Dehydrogenase activity and microbial biomass carbon in salt-affected soils of semiarid and arid regions. Arid Soil Research and Rehabilitation 11: 295–303.

Bompy, F., G. Lequeue, D. Imbert & M. Dulormne, 2014. Increasing fluctuations of soil salinity affect seedling growth performances and physiology in three Neotropical mangrove species. Plant and Soil 380: 399–413.

Boto, K. G. & J. T. Wellington, 1983. Phosphorus and nitrogen nutritional status of a northern Australian mangrove forest. Marine Ecology Progress Series 11: 63–69.

Boto, K. G. & J. T. Wellington, 1984. Soil characteristics and nutrient status in a Northern Australian mangrove forest. Estuaries 7: 61–69.

Bunt, J. S., W. T. Williams, J. F. Hunter & H. J. Clay, 1991. Mangrove sequencing: analysis of zonation in a complete river system. Marine Ecology Progress Series 72: 289–294.

Campo, J. T., M. Olvera-Vargas, B. L. Figueroa-Rangel, R. Cuevas-Guzmán & L. I. Iñiguez-Dávalos, 2018. Patterns of spatial diversity and structure of mangrove vegetation in Pacific West-Central Mexico. Wetlands. https://doi.org/10.1007/s13157-018-1041-6.

Cannicci, S., D. Burrows, S. Fratini, T. J. Smith III, J. Offenberg & F. Dahdouh-Guebas, 2008. Faunal impact on vegetation structure and ecosystem function in mangrove forests: a review. Aquatic Botany 89: 186–200.

Carter, M. R. & E. G. Gregorich, 2008. Soil sampling and methods of analysis. In Carter, M. R. & E. G. Gregorich (eds), Canadian Society of Soil Science, 2nd ed. CRC Press/Taylor & Francis Group, Boca Raton.

Centre for Science and Environment, India, 2012. Living with changing climate: impact, vulnerability and adaptation challenges in Indian Sundarbans. http://www.cseindia.org.

Chen, R. & R. R. Twilley, 1999. Patterns of mangrove forest structure and soil nutrient dynamics along the shark river estuary, Florida. Estuaries 22: 955–970.

Choudhury, A. M., 1968. Working Plan of Sundarban Forest Division for the Period from 1960-61 to 1979-80. East Pakistan Government Press, Tejgaon.

Cottam, G. & J. T. Curtis, 1956. The use of distance measures in phytosociological sampling. Ecology 37: 451–460.

Cruz, C. C. D., U. N. Mendoza, J. B. Queiroz, J. F. Berrêdo, S. V. D. C. Neto & R. J. Lara, 2013. Distribution of mangrove vegetation along inundation, phosphorus, and salinity gradients on the Bragança Peninsula in Northern Brazil. Plant and Soil 370: 393–406.

Cui, Y., L. Fang, X. Guo, X. Wang, Y. Zhang, P. Li & X. Zhang, 2018. Ecoenzymatic stoichiometry and microbial nutrient limitation in rhizosphere soil in the arid area of the northern Loess Plateau, China. Soil Biology and Biochemistry 116: 11–21.

Curnick, D. J., N. Pettorelli, A. A. Amir, T. Balke, E. B. Barbier, S. Crooks, F. Dahdouh-Guebas, C. Duncan, C. Endsor, D. A. Friess, A. Quarto, M. Zimmer & S. Y. Lee, 2019. The value of small mangrove patches. Science 363: 239.

Curtis, S. J., 1933. Working plan for the Sunderbans. Division Forest Department, Calcutta: 1931–1951.

Curtis, J. T. & R. P. McIntosh, 1950. The interrelations of certain analytic and synthetic phytosociological characters. Ecology 31: 434–455.

Datta, N. P., M. S. Khera & T. R. Saini, 1962. A rapid colorimeteric procedure for the determination of the organic carbon in the soil. Journal of the Indian Society of Soil Science 10: 67–74.

Deng, S. P. & M. A. Tabatabai, 1994. Cellulase activity of soils. Soil Biology and Biochemistry 26: 1347–1354.

Dinesh, R., S. G. Chaudhuri, A. N. Ganeshamurthy & S. C. Pramanik, 2004. Biochemical properties of soils of undisturbed and disturbed mangrove forests of South Andaman (India). Wetlands Ecology and Management 12: 309–320.

Dorich, R. A. & D. W. Nelson, 1983. Direct colorimetric measurement of ammonium in potassium chloride extracts of soils. Soil Science Society of America Journal 47: 833–836.

Elser, J. J. & A. Hamilton, 2007. Stoichiometry and the new biology: the future is now. PLoS Biology 5: e181.

Environment Agency, UK, 2010. The determination of easily liberated sulphide in soils and similar matrices. In: Methods for the Examination of Waters and Associated Materials: 10–17.

Etigale, E. B., S. Ajayi, S. I. Udofia & M. U. Moses, 2014. Assessment of stand density and growth rate of three tree species in an arboretum within the university of UYO, Nigeria. Journal of Research in Forestry, Wildlife and Environmental 6: 8–16.

Feller, I. C., 1995. Effects of nutrient enrichment on growth and herbivory of dwarf red mangrove (*Rhizophoramangle*). Ecological Monographs 65: 477–505.

Feller, I. C., D. F. Whigham, J. P. O'Neill & K. L. McKee, 1999. Effects of nutrient enrichment on within-stand cycling in a mangrove forest. Ecology 80: 2193–2205.

Feller, I. C., K. L. McKee, D. F. Whigham & J. P. O'Neill, 2003. Nitrogen vs. phosphorus limitation across an ecotonal gradient in a mangrove forest. Biogeochemistry 62: 145–175.

Freeman, C., N. Ostle & H. Kang, 2001. An enzymic 'latch' on a global carbon store. Nature 409: 149.

Friess, D. A., K. W. Krauss, E. M. Horstman, T. Balke, T. J. Bouma, D. Galli & E. L. Webb, 2012. Are all intertidal wetlands naturally created equal? Bottlenecks, thresholds and knowledge gaps to mangrove and saltmarsh ecosystems. Biological Reviews 87: 346–366.

Gallo, M., R. Amonette, C. Lauber, R. L. Sinsabaugh & D. R. Zak, 2004. Microbial community structure and oxidative enzyme activity in nitrogen-amended north temperate forest soils. Microbial Ecology 48: 218–229.

GESAMP (IMO/FAO/Unesco/WMO/WHO/IAEA/UN/UNEP Joint Group of Experts on the Scientific Aspects of Marine Pollution), 1991. Reducing Environmental Impacts of Coastal Aquaculture. GESAMP Reports and Studies, No. 47:35. Food and Agriculture Organization of the United Nations, Rome.

Gilman, E. L., J. Ellison, N. C. Duke & C. Field, 2008. Threats to mangroves from climate change and adaptation options. Aquatic Botany 89: 237–250.

Hutchings, P. & P. Saenger, 1987. Ecology of Mangroves. University of Queensland Press, St Lucia.

Huxham, M., M. P. Kumara, L. P. Jayatissa, K. W. Krauss, J. Kairo, J. Langat, M. Mencuccini, M. W. Skov & B. Kirui, 2010. Intra-and interspecific facilitation in mangroves may increase resilience to climate change threats. Philosophical Transactions of the Royal Society 365: 2127–2135.

Janzen, H. H., 1993. Soluble salts. In Carter, M. R. (ed.), Soil Sampling and Methods of Analysis. Lewis Publishers, Boca Raton: 161–166.

Joshi, H. & M. Ghose, 2003. Forest structure and species distribution along soil salinity and pH gradient in mangrove swamps of the Sundarbans. Tropical Ecology 44: 197–206.

Kandeler, E. & H. Gerber, 1988. Short-term assay of soil urease activity using colorimetric determination of ammonium. Biology and Fertility of Soils 6: 68–72.

Kettler, T. A., J. W. Doran & T. L. Gilbert, 2001. Simplified method for soil particle-size determination to accompany soil-quality analyses. Soil Science Society of America Journal 65: 849–852.

Kirwan, M. L. & J. P. Megonigal, 2013. Tidal wetland stability in the face of human impacts and sea-level rise. Nature 504: 53–60.

Krauss, K. W., C. E. Lovelock, K. L. McKee, L. López-Hoffman, S. M. L. Ewe & W. P. Sousa, 2008. Environmental drivers in mangrove establishment and early development: a review. Aquatic Botany 89: 105–127.

Krishnaswamy, U., M. Muthusamy & L. Perumalsamy, 2009. Studies on the efficiency of the removal of phosphate using bacterial consortium for the biotreatment of phosphate wastewater. European Journal of Applied Sciences 1: 6–15.

Kristensen, E., S. Bouillon, T. Dittmar & C. Marchand, 2008. Organic carbon dynamics in mangrove ecosystems: a review. Aquatic Botany 89: 201–219.

Langat, J. K. S., J. G. Kairo, M. Mencuccini, S. Bouillon, M. W. Skov, S. Waldron & M. Huxham, 2014. Rapid losses of surface elevation following tree girdling and cutting in tropical mangroves. PLoS ONE 10: e0118334.

López-Hoffman, L., N. P. R. Anten, M. Martinez-Ramos & D. D. Ackerly, 2007. Salinity and light interactively affect neotropical mangrove seedlings at the leaf and whole plant levels. Oecologia 150: 545–556.

Lovelock, C. E., M. C. Ball, B. Choat, B. M. J. Engelbrecht, N. M. Holbrook & I. C. Feller, 2006. Linking physiological processes with mangrove forest structure: phosphorus deficiency limits canopy development, hydraulic conductivity and photosynthetic carbon gain in dwarf *Rhizophora mangle*. Plant, Cell & Environment 29: 793–802.

Lugo, A. E., 1999. Mangrove ecosystem research with emphasis on nutrient cycling. In Yáñez-Arancibia, A. & A. L. Lara-Domínguez (eds), Ecosistemas de Manglaren América

Tropical. Instituto de Ecología A.C. México, UICN/ORMA, Costa Rica, NOAA/NMFS, Silver Spring: 17–38.
Lugo, A. E. & S. C. Snedaker, 1974. The ecology of mangroves. Annual Review of Ecology and Systematics 5: 39–64.
Marchand, C., F. Baltzer, E. Lallier-Vergès & P. Albéric, 2004. Pore-water chemistry in mangrove sediments: relationship with species composition and developmental stages (French Guiana). Marine Geology 208: 361–381.
McIntosh, J. L., 1969. Bray and morgan soil extractants modified for testing acid soils from different parent materials. Agronomy Journal 61: 259–265.
McKee, K. L., 1993. Soil physicochemical patterns and mangrove species distribution–reciprocal effects? Journal of Ecology 81: 477–487.
McKee, K. L., 1995. Seedling recruitment patterns in a Belizean mangrove forest: effects of establishment ability and physic-chemical factors. Oecologia 101: 448–460.
McKee, K. L., I. C. Feller, M. Popp & W. Wanek, 2002. Mangrove Isotopic (δ 15 N and δ 13 C) fractionation across a nitrogen vs. phosphorus limitation gradient. Ecology 83: 1065–1075.
Medina, E., 1984. Nutrient balance and physiological processes at the leaf level. In: Medina, E., H. A. Mooney, & C. Vázquez-Yánes (eds), Physiological Ecology of Plants of the Wet Tropics. Proceedings of an International Symposium held in Oxatepec and Los Tuxtlas, Mexico, June 29 to July 6, 1983: 139–154.
Medina, E., T. Giarrizzo, M. P. Menezes, M. L. Carvalho, E. A. Carvalho, A. Peres, A. B. Silva, R. Vilhena, A. Reise & C. Braga, 2001. Mangal communities of the "Salgado Paraense": ecological heterogeneity along the Bragança peninsula assessed through soil and leaf analyses. Amazoniana 16: 397–416.
Nickerson, N. H. & F. R. Thibodeau, 1985. Association between pore water sulphide concentrations and the distribution of mangroves. Biogeochemistry 1: 183–192.
Park, G., H. Oh & S. Ahn, 2009. Improvement of the ammonia analysis by the phenate method in water and wastewater. Bulletin of the Korean Chemical Society 30: 2032–2038.
Payo, A., A. Mukhopadhyay, S. Hazra, T. Ghosh, S. Ghosh, S. Brown, R. J. Nicholls, L. Bricheno, J. Wolf, S. Kay, A. N. Lázár & A. Haque, 2016. Projected changes in area of the Sundarban mangrove forest in Bangladesh due to SLR by 2100. Climatic Change 139: 279–291.
Reef, R., I. C. Feller & C. E. Lovelock, 2010. Nutrition of mangroves. Tree Physiology 30: 1148–1160.
Reise, A., D. Schories & E. Medina, 2010. Soil–vegetation nutrient relations. In Saint-Paul, U. & H. Schneider (eds), Mangrove Dynamics and Management in North Brazil, Vol. 11, 1st ed. Springer, Berlin: 91–107.
Rhoades, J. D., 1996. Salinity: electrical conductivity and total dissolved solids. In Sparks, D. L., et al. (eds), Methods of Soil Analysis, Part 3—Chemical Methods. SSSA Book Series No 5. SSSA and ASA, Madison: 417–436.
Sarker, S. K., R. Reeve, J. Thompson, N. K. Paul & J. Matthiopoulos, 2016. Are we failing to protect threatened mangroves in the Sundarbans world heritage ecosystem? Scientific Reports 6: 1–12.
Snedaker, S. C., 1982. Mangrove species zonation: why? In Sen, D. N. & K. S. Rajpurohit (eds), Contributions to the Ecology of Halophytes Tasks for Vegetation Science, Vol. 2. Springer, Dordrecht.
Sofawi, A. B., M. N. Nazri & M. Z. Rozainah, 2017. Nutrient variability in mangrove soil: anthropogenic, seasonal and depth variation factors. Applied Ecology and Environmental Research 15: 1983–1998.
Solórzano, L., 1969. Determination of ammonia in natural waters by the phenol hypochlorite method. Limnology and Oceanogrphy 14: 799–801.
The Hindu Business Line, 2012. Sundarbans' fragile ecology under threat from concrete embankments. Press Trust of India. https://www.thehindubusinessline.com/economy/Sundarbans%E2%80%99-fragile-ecology-under-threat-from-concrete-embankments/article20544533.ece. Accessed 21 Nov 2017.
Twilley, R. W., A. E. Lugo & C. Patterson-Zucca, 1986. Litter production and turnover in basin mangrove forests in southwest Florida. Ecology 67: 670–683.
Ukpong, I. E., 1997. Vegetation and its relation to soil nutrient and salinity in the Calabar mangrove swamp, Nigeria. Mangroves and Salt Marshes 1: 211–218.
Ukpong, I. E., 2000. Ecological classification of Nigerian mangroves using soil nutrient gradient analysis. Wetlands Ecology and Management 8: 263–272.
Valiela, I. & J. M. Teal, 1979. The nitrogen budget of a salt marsh ecosystem. Nature 280: 652–656.
Verchot, L. V. & T. Borelli, 2005. Application of *para*-nitrophenol (*p*NP) enzyme assays in degraded tropical soils. Soil Biology and Biochemistry 37: 625–633.
Vince, S. W. & A. A. Snow, 1984. Plant zonation in an Alaskan salt marsh: I. distribution, abundance and environmental factors. Journal of Ecology 72: 651–657.
Walter, H., 1971. Ecology of Tropical and Subtropical Vegetation. Oliver and Boyd, Edinburgh.
Ward, R. D., D. A. Friess, R. H. Day & R. A. MacKenzie, 2016. Impacts of climate change on mangrove ecosystems: a region by region overview. Ecosystem Health and Sustainability 2: e01211.
Whalen, J. K. & P. R. Warman, 1996. Arylsulfatase activity in soil and soil extracts using natural and artificial substrates. Biology and Fertility of Soils 22: 373–378.
Williams, W. T., J. S. Bunt & H. J. Clay, 1991. Yet another method of species-sequencing. Marine Ecology Progress Series 72: 283–287.
Wong, V. N. L., R. C. Dalal & R. S. B. Greene, 2009. Carbon dynamics of sodic and saline soils following gypsum and organic material additions: a laboratory incubation. Applied Soil Ecology 41: 29–40.